國立臺灣大學生命科學院生化科技學系

碩士論文

Graduate Institute of Biochemical Science and Technology
College of Life Science
National Taiwan University

Master Thesis

研究阿茲海默症中 TDP-43 與乙型類澱粉胜肽之間的分子交互作用

Understanding the Molecular Interaction of TDP-43 and Amyloid-β in Alzheimer's disease

陳容碩

Rong-Shuo Chen

指導教授：陳韻如 博士

Advisor: Yun-Ru Chen, Ph.D.

中華民國 108 年 7 月

July 2019

doi:10.6342/NTU201903526

誌謝

在兩年的碩士生涯中，我最感謝的就是陳韻如老師，從最一開始收我進實驗室當中研院暑期生、到當我實驗遭遇困難時指點我前進的方向，其間不斷鼓勵我實驗不如預期才有機會找到重大發現，在老師多重幫助與指導下，我才得以持續尋找解決問題的方法以及培養做實驗該有的好奇心與觀察力。另外，也非常感謝老師用心地營造實驗室歡樂的氛圍以及互相討論的風氣，讓我能在實驗室學長姐身上學到很多做實驗的技巧與態度。

接著要感謝最一開始指導我做實驗的方裕勝學長以及梁詩婕學姊，學長姐指導我各式做實驗的技巧，並帶領我熟悉各種儀器的操作與使用規則。另外要感謝賴煜升學長教導我如何設計實驗讓自己能夠更快做完，以及針對實驗結果的批判性思考和閱讀文獻的方法，這些對我培養做實驗的風格有著重要的影響。還要感謝張婷宇學姊、林天偉學長、施耀翔學長、蔡天穎學姊、張育仁學長、黃詩涵學姊和吳金潾學姊，學長姐們在指導與修正我做實驗的技巧上功不可沒。也感謝賴維斌學張、楊季樺學姊、陳仁偉學長、Kiki、林昕芃學妹、張明筠學姊和常健麟助理在平時給我許多幫助，讓我能更快融入實驗室中。

我要特別感謝江宛芹學姊，在我碩二下臨危受命，指導我完成我碩士論文中重要的實驗結果以及透過對於實驗中每個環節的提問，讓我能更進一步去思考實驗中每個步驟、材料和條件的用意，這對我撰寫本篇論文有很大的幫助。在碩士口試上，我要特別感謝吳偉銘學長、章微微學姊、莊靜玉學姊、張育仁學長和林芷瑄學姊，幫我指出故事不通順的地方以及指導我調整故事架構。

另外，也十分感謝我的口試委員，廖憶純老師、楊健志老師、杜玲嫻老師，以及我的指導教授陳韻如老師，在論文與口頭報告呈現上給予我很多實用的建議與思考方向。最後感謝我的家人以及我的女友，在我歷經實驗低潮時還是不斷支持我，給予我前進的動力，本篇獻給所有曾經幫助過我的人。

doi:10.6342/NTU201903526

中文摘要

漸凍人症的病理特徵，TDP-43 沉積，在阿茲海默症的病人中相當常見，這代表著 TDP-43 可能在阿茲海默症中是除了兩個為人所知的病理特徵乙型類澱粉蛋白 (Aβ)以及 tau 蛋白之外，第三個重要的病理特徵。根據陳韻如老師實驗室過去的研究結果，TDP-43 可以影響 Aβ40 的堆疊、使之保持在寡聚體的階段、並證實兩者間有交互作用，這些研究結果促使我想去探討 TDP-43 與 Aβ40 之間的分子交互作用。

首先，在 Thioflavin-T 檢測中，藉由讓特定幾個抗 TDP-43 寡聚體的單株抗體或市售的抗 TDP-43 的單株抗體與 TDP-43 結合，TDP-43 抑制 Aβ40 聚集的效能大幅降低，因此我發現 TDP-43 藉由其 N 端或是透過第二個與核糖核酸結合的位置(RRM2)和 Aβ40 產生交互作用。此外，雖然小鼠和人類的 TDP-43 主要差異在 RRM2 的序列，兩種蛋白都會影響 Aβ40 的堆疊。第二，在蛋白質核磁共振實驗中，我發現準備 Aβ40 所使用的緩衝液會造成 TDP-43 蛋白質構型改變，並可能進而使 TDP-43 無法和 Aβ40 有交互作用。但在改變 Aβ40 的準備方式後，我們仍發現氮 15 同位素標定的 TDP-43 N 端核磁共振圖譜並沒有發生改變，顯示在此條件下兩者無穩定作用。第三，在酵素免疫分析法中，藉由讓特定幾個抗 TDP-43 寡聚體的自製單株抗體或市售的抗 TDP-43 的單株抗體先與 TDP-43 結合，biotin-Aβ40 就無法或降低與 TDP-43 的結合，因此我發現 TDP-43 藉由其 C 端以及 RRM1+2 與 biotin-Aβ40 有交互作用。由此我們推測，Aβ40 與 TDP-43 有著多個交互作用的位置，確切位置仍需後續證明。

關鍵字：阿茲海默症、乙型類澱粉胜肽、TDP-43、蛋白質間交互作用、抗 TDP-43 寡聚體的單株抗體

doi:10.6342/NTU201903526

Abstract

ALS disease hallmarks, TDP-43 pathology, were rather common in Alzheimer's disease (AD), which suggested that TDP-43 might be the third important disease hallmarks in AD besides the well-known AD hallmarks, amyloid-β (Aβ) and tau protein. From the previous results of Dr. Yun-Ru Chen's lab, we found that TDP-43 could affect Aβ40 aggregation, retain it in its oligomeric state, and interact with it, which motivated me to investigate how did they interact in molecular level.

Firstly, in Thioflavin-T assay we demonstrated TDP-43 might interact with Aβ40 by its N-terminal or RNA recognition motif 2 (RRM2) region with the aid of selected self-prepared TDP-O antibodies and commercial antibodies. In addition, both mouse and human TDP-43 could affect Aβ40 aggregation although mouse TDP-43 mainly differed with human TDP-43 in RRM2 motif. Secondly, in ^{1}H-^{15}N HSQC protein NMR experiments we found that ^{15}N-Aβ40 preparation buffer altered TDP-43 conformation and might interrupt the interaction between ^{15}N-Aβ40 and TDP-43. But we still demonstrated no significant changes in N-terminal of ^{15}N-TDP-43 NMR graph after Aβ40 preparation was changed. The results showed that in the experimental condition, the two proteins did not stably interact. Thirdly, in ELISA assay, we demonstrated TDP-43 interacted with biotin-Aβ40 by its C-terminal or RRM1+2 domain with the aid of our TDP-O antibodies and the commercial antibodies. Our results suggested that Aβ40 could interact with multiple domains of TDP-43 and the specific interaction sites need further examination.

Keywords: Alzheimer's disease, amyloid-β, TDP-43, protein-protein interaction, monoclonal anti-TDP-43 oligomer antibody

doi:10.6342/NTU201903526

Contents

doi:10.6342/NTU201903526

doi:10.6342/NTU201903526

List of Figures

doi:10.6342/NTU201903526

doi:10.6342/NTU201903526

Chapter 1 Introduction:

1.1 Dementia:

According to WHO reports released in 2019, dementia patients worldwide have reached 50 million and the number increased at a rate of 10 million dementia patients every year. The reason why the number of people living with dementia keep increasing in modern world is due to longer lifespan attributed from the medical improvements. The longer we lived, the easier we get dementia because age is the major risk factor for dementia. Dementia would cause a deterioration in memory and thinking, which would lead to difficulties in recognizing family members, remembering ways to go home, and communicating with others. Therefore, dementia became a burden to people's living physically and psychologically and it also became a burden to their caregivers, families, and society[1]. The economic burden created by dementia was US$818 billion in 2015 and it was expected to grow to a US$ trillion in 2018 [2]. Due to its economic impact and no drugs available to cure dementia nowadays, WHO claimed dementia as a healthcare priority and needed global action to deal with it.

1.2 Alzheimer's disease

1.2.1 The discovery of Alzheimer's disease

The major diseases in dementia include Alzheimer's disease (AD), vascular dementia, dementia with Lewy bodies and frontotemporal dementia. Among these diseases, AD

doi:10.6342/NTU201903526

accounted for up to 60% to 70% of the cases, making it an important disease needed to be dealt with. AD was first described in 1906 by Dr. Aloysius Alzheimer to a 51-year-old woman patient. The description showed typical AD symptoms, including having difficulties in remembering recent events, reading, spelling, and communicating with other people. After the patient died, Dr. Aloysius Alzheimer performed silver staining histological technique to examine the patient's brain and found amyloid plaques were located extracellularly and neurofibrillary tangles were located in the cell. These disease hallmarks were recognized as Alzheimer's disease hallmark nowadays. People started to notice AD was in 1976 when Dr. Robert Katzman collected the number of people living with AD and concluded that the disease was the fourth leading cause of death in elderly people rather than a rare disease which was viewed by people at that time. This arose great attention from the National Institutes of Health and National Alzheimer's disease Research Center was established to study the cause, neuropathology, and clinical characteristics of AD. Due to intensive investigation, the criteria have been improved dramatically in differentiating different stages of AD, distinguishing AD from other neurodegenerative diseases and discovering biomarkers of AD [3].

1.2.2 Main hypothesis in AD and drug development

There were many hypothesis being proposed in order to describe the mechanism of AD [4]. The main two hypotheses were amyloid-beta (Aβ) cascade hypothesis and tau and tangle hypothesis because Aβ and hyperphosphorylated tau protein was the main components in the AD hallmarks. In Aβ cascade hypothesis, it proposed that the

doi:10.6342/NTU201903526

metabolism of Aβ changed gradually, allowing Aβ production increases and the clearance of Aβ decreases. It leads to Aβ oligomerization that increases severe and permanent changes to synaptic function [5-7]. Overtime, it caused inflammatory response, oxidative stress, progressive synaptic injury, hyperphosphorylation of tau protein and finally, widespread synaptic and neuronal dysfunction accompanied by cell death. Based on this hypothesis, over the years, Aβ peptides have been viewed as a potential drug target for AD [4].

Unfortunately, in the past few decades, both biotech and pharmaceutical companies could not found an effective drug to cure people living with AD. Lots of immunotherapy methods aiming to clear Aβ40 aggregate failed the phase III clinical trials. Nowadays, according to Alzheimer's Association, only five drugs approved by FDA could be used to treat AD patients. Three of them were cholinesterase inhibitors, which increased levels of neurotransmitter, acetylcoline, and help compensate for the loss of functioning brain cells. The fourth one was NMDA receptor antagonist, which could regulate the activity of glutamate by blocking NMDA receptors. The last one combined two drugs mentioned above into one treatment.

1.2.3 Aβ production and the structural characteristics

Aβ peptide was produced by amyloid precursor protein (APP) in its amyloidogenic pathway. APP was a transmembrane protein located on plasma membrane after its synthesis in the ER. If APP was cleaved by α-secretase in the plasma membrane, it goes to non-amyloidogenic pathway, in which no Aβ would be produced. If APP was cleaved by β-secretase in the plasma membrane or early endosome, which was preferable, it

doi:10.6342/NTU201903526

goes to amyloidogenic pathway, got cleaved by γ-secretase to produce Aβ peptide in the trans-Golgi network and the Aβ was secreted out of the cell [8]. The products of Aβ included 36 to 43 amino acids and the main Aβ products were Aβ40 and Aβ42. Aβ42 contained two more amino acids in the C-terminal compared Aβ40 and was much more aggregation-prone. Furthermore, Aβ42 was reported to be more toxic than Aβ40 and it was the main amyloid plaque in AD brain [9]. Aβ40 was reported to have higher concentration than Aβ42 in AD brain, could delay Aβ42 aggregation, and retain it in its soluble form for a longer time [10]. The structure of Aβ peptide monomer was commonly view as intrinsically unstructured and it might be the reason why it was hard to form crystal structure [11]. However, the fiber formed by Aβ was known as full of β-sheet structure solved by solid-state NMR [12].

1.3 TAR DNA-binding protein 43 (TDP-43)

1.3.1 The discovery of TDP-43

TDP-43 was first identified as a TAR DNA binding protein that played a role in regulating HIV-1 gene expression by altering or blocking transcription complex formation [13]. In the following studies, TDP-43 was found to play a more important role in mRNA splicing, transportation and translation [14]. The connection between TDP-43 and neurodegenerative disease was established by the identification that TDP-43 was a major component of the pathological hallmark in patients with amyotrophic lateral sclerosis (ALS) and frontotemporal lobar degeneration (FTLD) [15]. Further research showed that TDP-43 proteinopathy, including hyper-phosphorylation and

doi:10.6342/NTU201903526

depletion of TDP-43 from nucleus, was found in various major neurodegenerative diseases, including ALS, FTLD [16], AD [15], Parkinson's disease (PD) [17], and Huntington's disease (HD) [18].

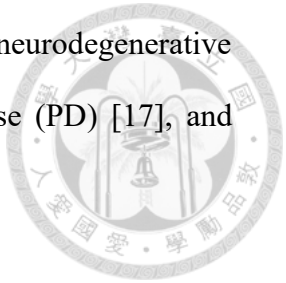

1.3.2 The physiological function of TDP-43

TDP-43 stands for TAR DNA-binding protein 43, which mainly locates in the nucleus in the cell and will shuttle to cytoplasm to perform physiological function. The normal biological function of TDP-43 is regulation of RNA pathway, including mRNA splicing in the nucleus, maintaining mRNA stability while transporting from nucleus to cytoplasm, and stress granule formation in the cytoplasm [19]. TDP-43 contains a N-terminal domain, a tandem RNA recognition motif and a flexible C-terminal (Fig. 1). The TDP-43 N-term is mainly responsible for dimerization, important for TDP-43 physiological function in RNA slicing, and prevents TDP-43 from aggregation [20]. The tandem RNA recognition motif in the middle of TDP-43 is responsible for UG-rich RNA recognition suggested by ^{1}H-^{15}N HSQC protein NMR [21]. The TDP-43 C-terminal region is a low complexity region, which lack constant conformation and secondary structures. However, it is the lack of constant conformation that gives it ability to interact with multiple hnRNP proteins that are important in mRNA splicing [22].

doi:10.6342/NTU201903526

1.3.3 The discovery and importance of TDP-43 in Alzheimer's disease

In Alzheimer's disease, TDP-43 pathology had been described in up to 50% of sporadic and 14% familial AD cases [23]. In two large clinical-pathologic cohorts, around a thousand participants brain autopsies were analyzed and TDP-43 pathology was present in almost two-thirds of the people diagnosed as Alzheimer's-type dementia, suggesting that mix pathologies of Alzheimer's disease and TDP-43 were more common than pathology of AD alone [24]. TDP-43 was reported that when phosphorylated TDP-43 accumulated in the cytoplasm, Tau mRNA became more stable and the expression of Tau or aggregation of Tau increased [23, 25]. TDP-43 was also reported to affect Aβ40 fibrillization, which retained Aβ40 in its oligomeric states [26]. These findings suggested that TDP-43 may play an important role in Alzheimer's disease.

1.3.4 The generation of monoclonal TDP-O antibodies

At first, the "A11" antibody, which was an anti-amyloid oligomer antibody, was used to investigate whether there were TDP-43 oligomers in ALS disease patients brain. However, the antibody could also recognize other amyloid oligomers like Aβ40 oligomers. To validate whether TDP-43 oligomers were presented in ALS patients, polyclonal anti-TDP-43 antibody was generated by Dr. Yu-Sheng Fang in our lab [26]. Rabbit was selected as the host and recombinant soluble TDP-43 was used as antigen. After using ELISA, size exclusion chromatography and dot blot, Dr. Yu-Sheng Fang

doi:10.6342/NTU201903526

successfully select an anti-TDP-43 oligomer antibodies, which help him validate TDP-43 oligomers existence in the patient brain.

The polyclonal antibody had a disadvantage of non-reproducible and it could obtain again only by sacrificing another host animal. In order to obtain stable reproducible anti-TDP-43 oligomer antibodies, monoclonal anti-TDP-43 oligomers antibodies were the best choices. Therefore, the recombinant human TDP-43 was purified again and act as an immunogen and Balb/c mouse was selected to become the host. The mouse was immunized with the immunogen following the standard protocol for monoclonal antibody production (LTK BioLaboratories, Taoyuan, Taiwan) by Dr. Wei-Wei Chang in our lab. After a series of experiments, eleven clones of monoclonal antibodies were selected and they were named as TDP-O1 to O11. These TDP-O antibodies were characterized by Dr. Wei-Wei Chang and found that TDP-O2 and TDP-O11 could recognize RRM1+2 region of human TDP-43 and TDP-O6 could recognize C-terminal of human TDP-43. Other TDP-O antibodies could not recognize any truncated forms of human TDP-43.

1.3.5 Possible extracellular and intracellular interaction between TDP-43 and Aβ40

TDP-43 might interact with Aβ peptide in the intracellular space including cytoplasm and mitochondria [27]. Mitochondria damage was associated with a range of neurodegenerative diseases, including AD and motor neuron disease (MND) [28]. Both TDP-43 and Aβ peptide were reported to locate in and caused damage to mitochondria,

doi:10.6342/NTU201903526

including reduced mitochondria membrane potential, elevated production of ROS, and reduced ATP synthesis [28, 29].

TDP-43 might interact with Aβ peptide extracellularly as well. Although physiological TDP-43 mainly located in the nucleus and pathological TDP-43 mainly located in the cytoplasm and form protein aggregates, the location of TDP-43 had also been reported to be in the exosome and was secreted by Neuro2a cells and primary neurons [30]. The excess levels of TDP-43 or TDP-43 protein aggregation were viewed as factors that could promote exosomal secretion of TDP-43. In the secreted exosomes, there were native soluble TDP-43 as well as truncated TDP-43. After enzyme cleavage, Aβ40 was secreted out of the cell. In the amyloid cascade hypothesis, it would start to form misfolded monomer, progress to oligomers, and finally form fibers. Due to exosomal secretion of TDP-43, TDP-43 would also be in the extracellular region, suggesting that TDP-43 may have a chance to interact with Aβ40 and retain it in its oligomeric form.

1.4 Aim of my research

Due to the prevalence of TDP-43 in Alzheimer's disease patients and the high association of TDP-43 pathology with clinical Alzheimer's-type dementia, it suggested that TDP-43 may play a role in Alzheimer's disease. Thanks to our lab members hard work, the interaction between TDP-43 and Aβ40 was confirmed by Octet and Aβ40 was retained in oligomeric state by TDP-43, which was elucidated by ThT assay and TEM (see Ting-Yu Chang master thesis).

In AD patients with TDP-43 pathology, they may have more severe AD-type dementia [31]. We proposed that it was because Aβ40 would be retained in oligomeric

doi:10.6342/NTU201903526

state by TDP-43, which was a more toxic to neurons than Aβ40 fibrils. If we could find the binding site between TDP-43 and Aβ40, we might have the ability to design drugs to block the interaction and retard the progression. Therefore, my research focused on understanding how TDP-43 interacts with Aβ40 in molecular level to find the binding site of these two proteins.

Several biophysical approaches are used to elucidate the interaction, including Thioflavin-T (ThT) assay, ^{1}H-^{15}N Heteronuclear Single-Quantum Coherence nuclear magnetic resonance of protein (^{1}H-^{15}N HSQC protein NMR), and enzyme-linked immunosorbent assay (ELISA). The reason why ThT assay is chosen is that when ThT binds to β-sheet rich structures that most amyloid aggregates have, it displays increased fluorescence and a red shift of its excitation and emission wavelength [32]. ThT dye is also commonly used in assays to find out the external factors that influence fibrillization of amyloid proteins [33-35]. ^{1}H-^{15}N HSQC protein NMR can elucidate the binding site between two proteins. The signals on ^{1}H-^{15}N HSQC NMR graph derived from ^{15}N and the hydrogen (^{1}H) on the ^{15}N in the protein backbone. Each residue in the protein had an amide except proline, which rendered each residue a signal in the ^{1}H-^{15}N HSQC NMR graphs. When two proteins interacted with each other, the microenvironment of the amide would change, indicating that the position on the NMR graph or the intensity of ^{15}N and the hydrogen (^{1}H) would change. In my research, ^{15}N labeled proteins with amino acid assignments were chosen in order to give the changed NMR signals meanings. ELISA can give the straightforward information whether the anti TDP-43 antibodies block the binding site between biotin-Aβ40 and TDP-43, which will be described in more detail in results section.

doi:10.6342/NTU201903526

Chapter 2 Material and methods

2.1 Protein expression and purification

2.1.1 TDP-43 (transactive response DNA binding protein 43 kDa)

Full-length human TDP-43 or TDP-43 (1-265) DNA sequence was inserted into pET14b vector. TDP-43 (1-100) and TDP-43 (101-265) DNA sequence was inserted into pQE30 vector. pET14b was transformed into *E.coli* rosetta 2 (R2) strain (Novagen, Merck KGaA) and pQE30 was transformed into *E.coli* M15 strain, which was a gift from Hanna S. Yuan, Institute of Molecular Biology, Academia Sinica. Full-length mouse TDP-43 DNA sequence was inserted into pQE80 vector and was transformed into *E.coli* M15 strain. Full-length human TDP-43 and TDP-43 (1-265) had a His tag and a linker in their N terminal, which contained MGSSHHHHHHSSGLVPRGSH-MLE residues. Full length mouse TDP-43, TDP-43 (1-100), and TDP-43 (101-265) had a His tag in their N terminal, which contained MRGSHHHHHHGS. *E.coli* was grown in LB broth and incubated at 37˚C, 200 rpm till $O.D._{600}$= 0.6 and 0.5 mM IPTG was added to induce protein expression. R2 strain was incubated at 16˚C and M15 strain was incubated at 18˚C for 20 hr. After twenty hours protein induction, *E.coli* was centrifuged at 5,000 rpm, 4˚C, 15 min to obtain pellet. The pellet was resuspended by 40 ml ddH_2O and centrifuged again at 8,000 rpm, 4˚C, 30 min in 50 ml falcon tube. The supernatant was discarded and pellet was preserved in -80˚C fridge. As for full-length TDP-43, R2 strain was grown in LB broth and incubated till $O.D._{600}$=0.4 and put into 4˚C cool room for 40 min to cool down. The *E.coli* was re-incubated at 16˚C, 200 rpm till $O.D._{600}$=0.6 and protein expression was induced by 0.5 mM IPTG. After twenty

doi:10.6342/NTU201903526

hours, the *E.coli* was harvested. The insoluble human and mouse full-length TDP-43 had a different incubation condition. After *E.coli* R2 strain or M15 strain were incubated at 37˚C till $O.D._{600}$=0.6, 0.5 mM IPTG was provided to induced protein expression. *E.coli* R2 strain or M15 strain were kept incubating at 37˚C for another 4 hr and *E.coli* was harvested.

The ^{15}N labeled TDP-43 (1-100) for NMR experiment was expressed in *E.coli* M15 strain using pQE30 expression vector. The media used was minimum M9 media, containing 6.78 g Na_2HPO_4, 3 g KH_2PO_4, 0.5 g NaCl, 0.01 mM $CaCl_2$, 2 mM $MgSO_4$, 0.004% glucose (freshly prepare), 1 g $^{15}NH_4Cl$ dissolved in 5 ml ddH_2O (freshly prepare), 50 μg/ml ampicillin and 25 μg/ml kanamycin. The *E.coli* M15 strain was incubated in minimum M9 media till $O.D._{600}$=0.6 and 0.5 mM IPTG was provided to induce ^{15}N TDP-43 (1-100) expression. After IPTG addition, the *E.coli* was incubated at 18˚C for 20 hr and it was harvested.

The *E.coli* pellet for soluble TDP-43 purificatoin was resuspended by lysis buffer, containing 30 mM Tris, 500 mM NaCl, 10% glycerol, 1 mM dithiothreitol (DTT), pH 8.0, 10 ng RNase, 10 ng DNase, and 100 μl protease inhibitor cocktail set III (EDTA-free, Roche Applied Science, Mannheim, German). *E.coli* was lysed by microfluidizer and centrifuged at 15,000 rpm, 4˚C, 30 min. The pellet was discarded and the supernatant was sterilized by 0.2 mm filter. Ni-NTA column was used to purify His-tag soluble protein and was first equilibrated by buffer A, including 30 mM Tris, 500 mM NaCl, 10% glycerol, 1 mM dithiothreitol (DTT), pH 8.0. The protein flew through Ni-NTA column and was washed by 20% buffer B, including 500 mM imidazole, 30 mM Tris, 500 mM NaCl, 10% glycerol, 1 mM DTT, pH 8.0. The protein was eluted by 20% to 60% gradient buffer B and protein purity was verified by 13% Tris-glycine SDS-

doi:10.6342/NTU201903526

PAGE. Pure full length TDP-43 and its truncated forms were stored at -20 ˚C fridge for further research.

The pellet of insoluble human and mouse full length TDP-43 was resuspended by lysis buffer, containing 50 mM Tris, 200 mM NaCl, 1 mM DTT, pH 8.0, 1 mg RNase, 1 mg DNase, and 100 µl protease inhibitor cocktail set III. After homogenized by vortex, the *E.coli* was lysed by microfluidizer and centrifuged to collect pellet. The pellet was resuspended by buffer C with the help of a stir bar. The resuspension was centrifuged at 20,000 rpm, 4˚C, 1 hr and supernatant was collected and sterilized by 0.2 mm filter. For insoluble human full-length TDP-43, the filtrate flew through the Ni-NTA open column three times. The open column was washed by 2% and 6% buffer D and the insoluble TDP-43 was eluted by 60% buffer D. The purity was verified by 13% Tris-glycine SDS-PAGE. The pure fractions were collected and concentrated to 200 µM using desalt buffer, containing 10 mM Tris, 6M urea, pH 8. The concentrated TDP-43 was allocated and stored at -20 ˚C fridge. For insoluble mouse TDP-43, the filtrate flew through commercial Ni-NTA column and the column was washed by 4% buffer D. Mouse TDP-43 was eluted by gradient of buffer D and the elution fraction of high concentration and low concentration were collected separately.

buffer A: 30 mM Tris, 500 mM NaCl, 10% glycerol, 1 mM DTT, pH 8.0.

buffer B: 500 mM imidazole, pH 8.0., 30 mM Tris, 500 mM NaCl, 10% glycerol, 1 mM DTT

buffer C: 50 mM Tris, 200 mM NaCl, 6 M urea, pH 8.0

buffer D: 50 mM Tris, 200 mM NaCl, 6 M urea, 500 mM imidazole, pH 8.0

doi:10.6342/NTU201903526

2.1.2 Aβ40 expression and purification

Materials:

The expression vector used was pET14b and the *E.coli* strain used was BL21 DE3*, which was purchased from Novagen (Merck, KGgA, Darmstadt, Germany). Isopropyl β-D-thiogalactopyranoside (IPTG) was obtained from Fisher Scientific (Pittsburgh, PA). Tobacco Etch Virus nuclear-inclusion-a endopeptidase (TEV protease) was a kind gift from one of lab members, doctor candidate Jin-Lin Wu. The pET14b-Aβ40 encoded a hexahistidine, *Xho*I cutting site and TEV protease recognition sequence "ENLYFQD" in the front of Aβ40 sequence.

Expression of His-tag Aβ40

After His-Aβ40 plasmid was transformed into *E.coli* BL21 DE3*, a single colony of *E.coli* BL21 DE3* was picked from 50 μg/ml ampicillin plate. It was inoculated in a 20 ml LB broth, containing 50 μg/ml ampicillin and the incubation condition was 37˚C, 200 rpm, 16 hr. All of the *E.coli* culture was poured into 1 L LB broth, containing 50 μg/ml ampicillin. The 1 L LB broth was incubated at 37˚C, 200 rpm until $O.D._{600}$ reach 0.8. and final concentration of 0.5 mM IPTG was provided to induce protein expression. After 18-20 hr of incubation at 37˚C, 200 rpm, cell was harvested by centrifuge at 5,000 rpm, 15 min, 4˚C and pellet was stored at -80˚C.

Purification of His-tag Aβ40

Pellet was resuspended by 20 ml lysis buffer, containing 20 mM Tris, pH 8.0, 150 mM NaCl with 1 mM DTT and lysed by a microfluidizer (M-110L, Microfluidics,

doi:10.6342/NTU201903526

Westwood, MA, USA). The cell lysate was centrifuged at 35,000 x g, 4˚C, 30 min and pellet was collected. Solubilization buffer A, containing 20 mM Tris, pH 12, 150 mM NaCl, 2 M urea, was used to resuspended pellet with the help of a stir bar. Resuspended pellet was sonicated for 1 hr at low temperature and centrifuged at 50,000 x g, 4˚C, 30 min. Supernatant was collected and sterilized through 0.2 or 0.4 mm filter. The Ni-NTA column was equilibrated by 6% buffer E, containing 20 mM Tris, pH 8.0, 150 mM NaCl, 5 M urea, 500 mM imidazole. Supernatant flew through the column. Then, the column was washed by 6% buffer E in 15 column volume and His-tag Aβ40 was eluted by gradient from 6% to 100% buffer E in another 15 column volume. The purity of His-tag Aβ40 was verified by 13% Tris-tricine SDS-PAGE.

Cleavage of His-tag Aβ40

The pure His-tag Aβ40 fractions were concentrated by 3 kDa cut-off centricon to 1 ml and the concentration was determined by nanodrop with the extinction coefficient of 2,560 $M^{-1}cm^{-1}$, which was calculated from two tyrosine residues in the recombinant protein, and molecular weight of 7.17 kDa. Lysis buffer mentioned above was added to dilute urea concentration to 1 M, which allowed TEV enzyme to cleave the TEV recognition site, including His-tag, in front of Aβ40 sequence. The ratio of TEV enzyme to His-tag Aβ40 was 1 to 100. The condition was in the water bath with temperature at 30˚C and the reaction time was 16 to 20 hr.

Purification of Aβ40 without His-tag

Solubilization buffer B, containing 20 mM Tris, pH 8.0, 150 mM NaCl, 8 M urea was added into the post proteolysis products to inactivate TEV enzyme and bring the

doi:10.6342/NTU201903526

concentration of urea back to 5 M, which was aim to prevent Aβ40 aggregation. The inactivation process took 1 hr and the sample was concentrated by 3 kDa cut-off centricon till the volume reached 5 ml. The purification process repeated again. This time Aβ40 without his-tag should be in the flow through.

Reverse Phase - HPLC

The pure Aβ40 fractions were collected and concentrated by 3 kDa cut-off centricon till the volume reached 1 ml. Centrifugation at 17,000xg, 4 ℃ for 10 min was applied to remove any Aβ40 aggregation formation. The supernatant was collected and 100% acetonitrile, ACN for short, was added into the supernatant to reach 30% ACN. The mixture was sonicated for 10 min and centrifuged for another 5 min, 4 ℃, and 15,000 rpm. The HPLC column was Jupiter 4 μm Proteo 90 angstroms with scale of 250 x 10 mm (Phenomenex, US). The column was first equilibrated by buffer F, containing 20% ACN, 0.05% TFA and the purification program was run without any sample in it to check to condition of the column. If no issue arose, Aβ40 sample with 30 % ACN was injected through the HPLC column at 3 ml/min. The program was designed as the following. The 100% buffer F was used to help Aβ40 flow through HPLC column and wash out other small molecules in Aβ40 solution in 10 min at a rate of 3 ml/min. A gradient was applied to eluted Aβ40 from 0% to 100% of buffer G, containing 90% ACN, 0.05% TFA within 30 min. It took 10 min of 100% buffer G to wash out any protein in the column and it took another 10 min of buffer G gradient to make sure all the protein was washed out. Finally, it took 10 min of buffer F to equilibrate the column and prepare for the next run.

doi:10.6342/NTU201903526

The volume of 10 μl was taken from the elution fraction and matrix-assisted laser desorption/ionization time of flight/ time of flight (MALDI TOF/TOF) was used to verify the m/z value of Aβ40 from HPLC elution fractions. The pure Aβ40 fractions were collected and freeze-dry to remove organic compound. The Aβ40 powder was weighted, allocated into 1mg per Eppendorf by 50% ACN, and stored in -80 ℃ fridge with Eppendorf cap that was sealed by Parafilm.

buffer E, containing 20 mM Tris, pH 8.0, 150 mM NaCl, 5 M urea, 500 mM imidazole
buffer F, containing 20% ACN, 0.05% TFA
buffer G, containing 90% ACN, 0.05% TFA

2.2 dot blot

Insoluble human and mouse TDP-43 was quantified by UV 280 and diluted by buffer to 4 μM. If TDP-43 was diluted by buffer D to maintain denature condition, it was denoted as "1". On the contrary, if TDP-43 was diluted by 10 mM Tris, pH 8.0 to refold, it was denoted as "2". If 2% SDS was introduced, TDP-43 was in "S" column compared to no SDS column, which was denoted as dash. All the labels were written in Fig. 12B. After all samples were prepared, 2 μl of each sample was introduced to nitrocellulose membrane and samples were allowed to dry overnight. The dry membranes were incubated in 5% skim milk in TBS-T to block all possible binding site on NC membrane for 2 hr. The milk was discarded and the membranes were washed by TBS-T three times and incubated in 5% skim milk containing monoclonal anti-TDP-43 antibodies produced by Dr. Yun-Ru Chen's lab, abbreviated as TDP-O1 to O11 in a ratio of 1 :

doi:10.6342/NTU201903526

1,000 for 2 hr. Commercial anti-TDP-43 antibodies, 2E2D3 and 10782, were added in a ratio of 1 : 5,000 within 5% skim milk. The antibodies were discarded and the membranes were washed by TBS-T three times. All membranes were incubated in 5% skim milk containing secondary antibody, anti-mouse antibody, in a ratio of 1 : 10,000 for 2 hours. The secondary antibody was discarded and the membranes were washed again. The substrate ECL (Millipore, immobilon R Western) was added and the photos were taken in chemiluminescent manner.

2.3 Size exclusion chromatography

Superdex-200 column was standardized by Dr. Yu-Sheng Fang through markers provided by GE Healthcare. Insoluble human TDP-43 was dialyzed in 10 mM glycine, pH 2.7 twice, the supernatant was collected and quantified by microBCA assay. The volume of 500 μl TDP-43 was injected into the column and the buffer used was also 10 mM glycine, pH 2.7. The flow rate was 0.3 ml/min and the temperature was 4℃. All the fractions were checked by SDS-PAGE.

2.4 Western blot

The monomer fraction of human TDP-43 based on previous standardization was obtained from size exclusion chromatography. The monomer TDP-43 was further denatured by sample buffer addition, containing 50% glycerol, 0.325 M Tris-HCL, pH 6.8, 12.5% SDS, and 25% β-mercaptolethanol, and by heat at 95 ℃, 10 min. The denature TDP-43 was loaded into separate wells in SDS-PAGE flanked by markers.

doi:10.6342/NTU201903526

After gel electrophoresis was done, the proteins on SDS-PAGE were transferred to nitrocellulose membrane at 250 mA and 75 min. The nitrocellulose (NC) membranes were cut into thirteen pieces to allow thirteen different antibodies to be tested. The NC membranes were blocked by 5% skim milk and washed by TBS-T in the same manner as dot blot. The TDP-O primary antibodies and commercial anti-TDP-43 antibodies, 2E2D3 and 10782, were added in the concentration of 2 μg. The secondary antibodies were added in a ratio of 1 : 10,000. The substrate ECL detection kit was used and the photos were obtained in chemiluminescent manner.

2.5 Thioflavin T assay

The 1 mg Aβ40 powder was allocated by 50% ACN into 0.1 mg per Eppendorf after it was sonicated for 10 min to prevent aggregation formation. The 0.1 mg Aβ40 powder was treated by 100 μl hexafluoro-2-propanol (HFIP) and sonicated for 10 min to monomerize Aβ40. The Aβ40 solution stayed at RT for at least 2 hr before freeze-dry overnight. At the same day, full-length human or mouse TDP-43 was dialyzed in 10 mM Tris, pH 8.0 twice. In the next day, centrifugation at 13,300 rpm, 4 ℃, 10 min was applied to full-length human or mouse TDP-43 in order to remove precipitates after dialysis. The supernatant was obtained and quantified by microBCA assay. Both of the human and mouse full-length TDP-43 was concentrated by Ultra-0.5 10 kDa cut-off centricon to the desired concentration. In the experiment aiming to find the binding site between human TDP-43 and Aβ40, human TDP-43 was concentrated to 1 μM and equimolar or 1 nM of anti-human TDP-43 antibodies were mixed with full-length human TDP-43 in the same volume respectively. The mixture of full-length human

doi:10.6342/NTU201903526

TDP-43 and anti-human TDP-43 antibody were incubated at RT for 3 hr to allow the interaction to happen. The aliquot of 0.1 mg Aβ40 powder was dissolved in 4 μl of 100% dimethyl sulfoxide (DMSO) and added into 96 μl TDP-43 dialysis buffer, containing 10 mM Tris, pH 8.0, in a slowly spiral way. Centrifugation at 13,300 rpm, 4 ℃, 10 min was applied to Aβ40 solution and supernatant was quantified by BCA assay. The better concentration of Aβ40 in ThT assay was 25 μM, the concentration of human TDP-43 was 0.25 μM, and the concentration of ThT was 5 μM. Full-length human TDP-43 alone or the mixture of full-length human TDP-43 and anti-human TDP-43 antibody were added into Aβ40 solution to reach 0.25 μM of TDP-43 and equal-molar, 0.25 nM, or 0.05 μM of anti-human TDP-43 antibody if it was included. The mixture of Aβ40, full-length human TDP-43 and / or anti-human TDP-43 antibody were added into 384-well standard opaque ELISA plate in 3-repeat manner and the incubation condition was no-shaking. After an hour incubation was reached, ELISA plate would shake for 1 min. The ThT intensity was detected after the ELISA plate shaking and the excitation and emission wavelength was 442 nm and 485 nm respectively.

2.6 ^{1}H-^{15}N Heteronuclear Single-Quantum Coherence (HSQC)

nuclear magnetic resonance of protein (protein NMR)

2.6.1 ^{15}N labeled Aβ40

^{15}N labeled Aβ40 peptide was purchase from rPeptide Company. ^{15}N labeled Aβ40 was allocated in the same manner as Aβ40 without ^{15}N label. The freeze-dry of 0.1 mg

doi:10.6342/NTU201903526

^{15}N labeled Aβ40 was dissolved by 5 μl 8 M GdnHCl (in pH 7.4 Tris) and refolded in 95 μl NMR buffer, including 50 mM Tris, pH 6.8, 20 mM NaCl. ^{15}N Aβ40 solution was centrifuged at 13,300 rpm, 4˚C, 10 min and the supernatant was quantified by BCA assay. The working concentration of ^{15}N Aβ40 was different depending on which TDP-43 variants was used. TDP-43 variants were dialyzed in NMR buffer twice and centrifuged at 13,300 rpm, 4˚C, 10 min. The supernatant was quantified by BCA assay. The final volume of protein mixture was 250 μl containing 10% D_2O and protein mixture would be added into a NMR tube (Shigemi Inc., Allison Park, PA, USA). The NMR graph was recorded on 600 or 850 MHz NMR spectrometer and the temperature used most of the time was 278K (5 ℃) to avoid Aβ40 aggregation in the process of experiments.

2.6.2 ^{15}N labeled TDP-43 (1-100)

^{15}N labeled TDP-43 (1-100) was dialyzed in NMR buffer, including 50 mM Tris, pH 6.8, 20 mM NaCl twice and centrifuged at 13,300 rpm, 4˚C, 10 min. The pellet was discarded and the supernatant was quantified by BCA assay. The protein was concentrated by 3 kDa cut-off centricon and quantified again by BCA assay. The working concentration of ^{15}N TDP-43 (1-100) was 50 μM or 25 μM in around 250 μl with 10% D_2O included. Every 0.1 mg of Aβ40 powder was denatured by 5 μl 8 M GdnHCl and refolded in 95 μl NMR buffer. Aβ40 was centrifuged at 13,300 rpm, 4˚C, for 10 min and supernatant was quantified by BCA assay. In the experiments, it was Aβ40 without ^{15}N labeled that was added into ^{15}N TDP-43 (1-100). Before protein was added into a NMR tube, their pH value would be detected by pH meter. The NMR

doi:10.6342/NTU201903526

experiments were recorded on 600 MHz NMR spectrometer equipped with ^{1}H, ^{15}N TCI Cryo probe and were performed at pH 6.8 at 298K (25 ℃).

2.7 ELISA

The allocation of 1 mg biotin-Aβ40 was the same as Aβ40. The difference was that after HFIP treatment, 0.1 mg biotin-Aβ40 was dissolved in 100 μl of 3 mM NaOH and sonicate for 2 min and froze dry. At the same day, 20 μl, 200 μM insoluble TDP-43 was added into 5 ml 10 mM Tris, pH 8. to refold. In order to remove the urea completely, desalt method was applied. Ultra-15 centricon was used and 10 mM Tris, pH 8 was acted as desalt buffer. After the concentration of urea was lowered to pico-molar level, the concentration of refolded TDP-43 was quantified by BCA assay. The required concentration of refolded TDP-43 was coated on ELISA plate with a lad on the top and the incubation condition was 4 ℃, 60 rpm, overnight.

The refolded TDP-43 was discarded and each well was blocked by 200 μl 2% BSA or 2.5% skim milk in PBS-T, containing 0.137 M NaCl, pH 7.4, 2.7 mM KCl, 0.01 M Na_2HPO_4, 1.8 mM KH_2PO_4, 0.005% tween, for 2 hr on a 2D shaking plate. After blocking, 2% BSA or 2.5% skim milk was removed and the ELISA plate was washed by PBS-T four times. Anti-TDP-43 antibody was added into each well in PBS-T with 1% BSA or 2.5% skim milk. The plate was incubated at RT 2 hr. The antibody solution was discarded and the ELISA plate was washed by 200 μl PBS-T four times. Biotin-Aβ40 was dissolved in 200 μl PBS and centrifuged at 4 ℃, 13,300 rpm, for 10 min. The supernatant was quantified by BCA assay. Biotin-Aβ40 with required concentration was added into ELISA plate and incubated at RT for 2 hr. The biotin-

doi:10.6342/NTU201903526

Aβ40 was discarded and the ELISA plate was washed by PBS-T four times. Streptavidin-HRP (SA-HRP) was diluted at 1:5,000 by PBS-T with or without 1% BSA, added into each well, and incubated 1 hr. The SA-HRP solution was discarded and PBS-T was used to wash the ELISA plate twice. 3, 3', 5, 5'-tetramethylbenzidine, TMB substrate for short, with 100 μl was added into each well and incubated for 3 min. The concentration of 0.25 M HCl was added to stop the reaction in the same volume as TMB substrate. The ELISA plate was first shaken by ELISA plate reader for 10 sec and the absorbance of two wavelength was detected, which was 450 nm and 630 nm.

doi:10.6342/NTU201903526

Chapter 3 Results

3.1 Protein purification

3.1.1 Full-length and truncated human TDP-43

The cartoon of full-length human TDP-43 and its truncated forms were shown in Fig. 1. Soluble full-length TDP-43 and TDP-43 (1-265) was transformed into *E.coli* rosette 2 strain via pET14b expression vector. Soluble TDP-43 (1-100) and TDP-43 (101-265) was transformed into *E.coli* M15 strain via pQE30 expression vector. The different *E.coli* strains except for soluble full-length human TDP-43 were incubated in LB broth till $O.D._{600}$ = 0.6 and 0.5 mM IPTG were added. Since using the condition mentioned above to incubate full-length human TDP-43, there were lots of truncated TDP-43 after purification (Fig. 3B). Therefore, I used a different expression protocol to get full-length human TDP-43, ~47 kDa. It was incubated in LB broth till $O.D._{600}$ = 0.4, cooled down to 16˚C, kept incubated at 16˚C till $O.D._{600}$ =0.6 and added with 0.5 mM IPTG. After 16~18 hour of IPTG induction, the cells were harvested. The pellet of soluble full-length human TDP-43 was resuspended by 100 ml lysis buffer and lysed by microfluidizer. The lysate was centrifuged and supernatant was obtained. After equilibrated by 20 mM imidazole, the supernatant was injected through Ni-NTA column (Fig. 4A upper panel). The Ni-NTA column was washed by 75 mM and 100 mM imidazole at least 10 column volumes respectively and eluted by gradually increasing imidazole concentration from 100 to 300 mM (Fig. 4A lower panel). The purity of the protein was checked by 13% SDS-PAGE (Fig. 4B) and the full-length

doi:10.6342/NTU201903526

TDP-43 was observed at ~48 kDa position in lane 40 to 48 (Fig. 4B right panel). The fractions for lane 42 to 45 were collected.

For insoluble human and mouse full-length TDP-43, the pellet was resuspended by its specific lysis buffer, containing 50 mM Tris, pH 8.0, 200 mM NaCl, and the cell was lysed by microfluidizer. The lysate was centrifuged and the pellet was collected. The pellet was resuspended by buffer C mentioned in methods, containing 6 M urea. The protein content of lysate and resuspended pellet was shown in SDS-PAGE in Fig. 5 in lane L and lane P. It showed that when the incubation method changed, most TDP-43 was in the pellet part of the cell lysate and needed 6 M urea to solubilize them. After second centrifugation, the supernatant was collected and went through 0.22 nm filter to make sure no large cell debris remained in the supernatant. The supernatant of insoluble human full-length TDP-43 was injected into Ni-NTA open column separately for three times and the column was washed by the mixture of buffer C and D with 10 mM and 30 mM imidazole, which were denoted as W1 and W2 in Fig. 5. The insoluble human full-length TDP-43 was eluted by the mixture of buffer C and D with 300 mM imidazole, which was denoted as E1 to E8 in Fig. 5. Although there were truncated form of TDP-43 observed in elution region, the bands of full-length TDP-43 were much larger than the truncated one, indicating that after dilution, the concentration of truncated TDP-43 was neglectable. All the elution fractions were collected. The supernatant of insoluble mouse full-length TDP-43 was injected into Ni-NTA commercial column and the column was washed by the mixture of buffer C and D (Fig. 6A). The insoluble mouse full-length TDP-43 was eluted by gradient of buffer D, the elution fraction was collected, and they were denoted as lane 11 to lane 19 in SDS-PAGE (Fig. 6B). The

doi:10.6342/NTU201903526

high concentration and low concentration of mouse full-length TDP-43 were collected separately.

For soluble truncated TDP-43 (1-265), the purification procedure was mentioned in method. In brief, after the lysate was centrifuged, it was equilibrated with 4% buffer B and injected through Ni-NTA column with the volume of 40 ml. The column was washed by 20% buffer B for 10 column volumes and the protein was eluted by gradually increasing percentage of buffer B (Fig. 7A). The purity was checked by 13% SDS-PAGE and the elution fractions with single band at ~30 kDa were collected (Fig. 7B). For soluble truncated TDP-43 (101-265), the purification processes were the same as truncated TDP-43 (1-265). However, the it had a lower affinity to Ni-NTA column than truncated TDP-43 (1-265), which led to instant elution when imidazole concentration increased to 100 mM. The stage was the wash step for TDP-43 (1-265) purification. The chromatograph in Fig. 8A showed the instant elution and the SDS-PAGE in Fig. 8A right panel lane 13 indicated that TDP-43 (101-265) was eluted and the target protein was still mixed with other proteins. Therefore, the fraction was diluted till the concentration of imidazole decreased to around 20 mM and purify again (Fig. 8B, left panel). This time, the concentration of imidazole was increased gradually from 20 mM to 300 mM in order to wash out low-affinity proteins and elute target proteins. The purity of eluted protein was checked by 13% SDS-PAGE (Fig. 8B, right panel). The band of truncated TDP-43 (101-265) was at lane 17 to 26 in Fig. 8B and lane 17 to 20 were collected. For truncated TDP-43 (1-100) and its ^{15}N labeled counterparts, the purification method had a little difference in column washing step but other steps were the same (Fig. 9A & 10A). The elution region was checked by 13% SDS-PAGE and the selected part was collected (Fig. 9B & 10B).

doi:10.6342/NTU201903526

3.1.2 Aβ40 purification

The sequence of His-Aβ40 contained six histidine repeats, a TEV cutting site, and protein sequence of Aβ40, which rendered the molecular weight of Aβ40 to 7.3 kDa. After Aβ40 was purified followed the steps described in method, the purity of it was checked by Tris-tricine step gradient SDS-PAGE (Fig. 11B, left panel). After the concentration was determined by nanodrop, the required concentration of TEV was added into diluted His-Aβ40 solution, which allowed TEV to retain its enzyme activity. After His-tag was cleaved, Aβ40 was purified again and the flow through fraction was collected. The purity was also checked by Tris-tricine step gradient SDS-PAGE (Fig. 11B, right panel), which indicated Aβ40 without His-tag was purified because it had a smaller molecular weight. The purified Aβ40 was concentrated and had a third purification by reverse phase HPLC (Fig. 11C). There were two peaks in the HPLC chromatogram. The first peak, which appeared early in the chromatogram, did not contain Aβ40 whose theoretical m/z value was 4330 (Fig. 11D). The second peak was also checked by MALDI-TOF/TOF (Fig. 11C right panel) and the m/z value was similar to Aβ40 theoretical m/z value. Therefore, the elution fractions were collected.

3.1.3 Characterization of monoclonal anti-human TDP-43 oligomer antibodies

To characterize monoclonal anti-human TDP-43 oligomer antibodies, which were abbreviated as TDP-O1 to TDP-O11, produced by Dr. Wei-Wei Chang in Dr. Yun-Ru

doi:10.6342/NTU201903526

Chen's lab, insoluble human and mouse full-length TDP-43 were used. In order to test different characteristics of TDP-O antibodies, dot blot method was used (Fig. 12). First, to test whether TDP-O antibodies could recognize refolded human and mouse TDP-43, TDP-43 was refolded in 10 mM Tris, pH 8.0 by direct dilution. As a negative control, TDP-43 was diluted to the same concentration by buffer C containing 6 M urea. To further test whether TDP-O antibodies could recognize monomer form of TDP-43, 2% SDS was used, which was denoted as a single letter "S". All the label was put in Fig. 12B. In Fig. 12A and Fig. 12C, TDP-O2, O6 could recognize mouse TDP-43 in both denature or refold condition, which was labeled in 1 and 2 in Fig. 12B. TDP-O1, O5, O8, and O10 could recognize mouse TDP-43 in denature form but could not recognize mouse TDP-43 in its refolded condition. On the other hand, all TDP-O except TDP-O7 could recognize human TDP-43 in its refolded form and denature form. No TDP-O antibodies except TDP-O6 might recognize mouse TDP-43 after 2% SDS was added (Fig. 12C). As for human TDP-43, TDP-O2, O6, and O11 could recognize it after 2% SDS was added, indicating that only TDP-O2, O6, and O11 could recognize monomer human TDP-43. Commercial monoclonal anti-TDP-43 antibody 2E2D3, which recognized TDP-43 (205-222) region and commercial polyclonal anti-TDP-43 antibody 10782, which recognize TDP-43 (1-260) region were used as positive control (Fig. 12D). Monoclonal anti-TDP-43 (205-222) antibody could differentiate human TDP-43 from mouse TDP-43 because the recognition site happened to be the place where human and mouse TDP-43 had the biggest protein sequence differences (Fig. 2). On the contrary, polyclonal anti-TDP-43 (1-260) antibody could not differentiate human and mouse TDP-43.

doi:10.6342/NTU201903526

To further confirm that only TDP-O2, O6, and O11 could recognize monomer human TDP-43, insoluble TDP-43 was first dialyzed in 10 mM glycine, pH 2.7, to obtain a denature form of TDP-43. Then, TDP-43 was injected into size exclusion column and all the fractions were run in the SDS-PAGE (Fig. 13A and 13B). The monomer fraction, which was fraction 15, was picked and western blot was performed. TDP-O antibodies were used separately and the results showed that only TDP-O2, O6, and O11 could recognize monomer human TDP-43 (Fig. 13C). Commercial anti-TDP-43 antibodies, 2E2D3 and 10782, were used as positive controls.

3.2 Examination of interactions between TDP-43 and Aβ40

From our previous lab members' attributions, we knew that TDP-43 interferes the fibrils formation of Aβ40, causing Aβ40 to form oligomers rather than fibers (25). We also knew that Aβ40 would bind to full-length TDP-43 and truncated TDP-43 variants, except TDP-43 (1-100) due to non-specific binding to streptavidin probe used in Octet experiments (unpublished data). Here, in order to investigate the interaction between Aβ40 and TDP-43, several biophysical approaches were used, including Thioflavin-T (ThT) assay, nuclear magnetic resonance (NMR), and enzyme-linked immunosorbent assay (ELISA).

doi:10.6342/NTU201903526

3.2.1 ThT assay

3.2.1.1 ThT assay of Aβ40 and TDP-43 in the presence or absence of anti-TDP-43 antibodies

In order to test how Aβ40 performed in ThT assay, I tried two concentrations, which were 15 μM and 25 μM at pH 8.0 in 10 mM Tris (Fig. 14A). It showed that when Aβ40 was 25 μM, the aggregation progress was much better than it was 15 μM. Therefore, the concentration of Aβ40 was chosen. In order to investigate whether the protein sequence difference between human and mouse TDP-43 affect Aβ40 aggregation, both of them were dialyzed in 10 mM Tris, pH 8. The concentration of both human and mouse full-length TDP-43 was limited to 0.25 μM because of low concentration after dialysis. Although the concentration of Aβ40 was 100-fold of both full-length TDP-43, both of them still interfere Aβ40 aggregation. Decreased Aβ40 ThT fluorescent intensity was observed when Aβ40 and TDP-43 were incubated together (Fig. 14B). Full-length human TDP-43 may have interaction with Aβ40, which causes it to stay at its oligomeric state or other states except forming β-sheet rich fibril structures. Mouse TDP-43 also could inhibit Aβ40 aggregation, suggesting the protein sequence difference in human and mouse TDP-43 may not affect it to interact with Aβ40. Because Alzheimer's disease was mainly a human disease, I chose human TDP-43 and Aβ40 as my main research targets.

In order to investigate the binding site between human TDP-43 and Aβ40, anti-human TDP-43 antibodies were applied to bind to human TDP-43 first through pre-incubation

doi:10.6342/NTU201903526

and the mixtures were added into Aβ40 solution. If anti-human TDP-43 antibody blocks the binding site between human TDP-43 and Aβ40, Aβ40 would be relieved from the inhibition of human TDP-43 and aggregated freely. Because human TDP-43 was mostly oligomers, TDP-O antibodies and purchased anti-human TDP-43 antibodies were used in equal-molar to human TDP-43 to block the possible Aβ40 binding site (Fig. 14C). The epitope of TDP-O antibodies was characterized previously by Dr. Wei-Wei Chang (unpublished data). They are TDP-O6, which bond to C-terminal of TDP-43; and TDP-O11, which bond to RRM1+2 domain of TDP-43. The purchased anti-human TDP-43 antibodies included anti-TDP-43 (1-103) and anti-TDP-43 (205-222). Monoclonal antibody to G2a, IgG2a for short, was used as a negative antibody control, for it was the isotype of TDP-O antibodies and it was commonly used to test the non-specific binding to mouse IgG antibody. In Figure 14C, no matter TDP-43 incubated with IgG2A, TDP-O6, or TDP-O11, they all showed superior suppression on Aβ40 aggregation due to unknown reason compared to TDP-43 effect on Aβ40. When TDP-43 incubated with commercial antibodies, anti TDP-43 (1-103) and anti TDP-43 (205-222), the lag phase of Aβ40 aggregation was shortened and the intensity of Aβ40 was enhanced.

Concerning the high concentration of antibodies that may influence Aβ40 aggregation, the concentration was adjusted to 1,000-fold lower than TDP-43 (Fig. 15). The behavior of Aβ40 and the effect of TDP-43 on Aβ40 was consistent in Fig. 15A. The purchased antibodies were chosen, for the production might be more stable and they enhanced Aβ40 aggregation, which indicated that they may have blocked the binding site between Aβ40 and TDP-43. After the low concentration of antibodies co-incubated with TDP-43 and added into Aβ40 solution, Aβ40 aggregation process was rescued to some degree.

doi:10.6342/NTU201903526

The lag phase of Aβ40 aggregation was shortened compared to co-incubation of Aβ40 and TDP-43 and the intensity was restored or even higher than Aβ40 alone. (Fig. 15A). To make sure the phenomena were due to the interruption of TDP-43 and Aβ40 interaction, Aβ40 was also incubated with anti-TDP-43 antibodies alone as a negative control (Fig. 15B). It showed that the antibodies didn't interfere with Aβ40 aggregation significantly, which suggested that it was the rescue effect which anti-human TDP-43 antibodies bond to TDP-43 that allowed Aβ40 to aggregate without TDP-43 disruption. When the concentration of anti-human TDP-43 antibodies increase to 0.05 μM, Aβ40 aggregation was fully rescued (Fig. 15C). Although co-incubation of Aβ40 and anti-TDP-43 antibody had a higher intensity than Aβ40 alone, the lag phase was the same, indicating that the high concentration of anti-TDP-43 antibodies did not affect Aβ40 aggregation pathway (Fig. 15D). This supported TDP-43 interact with Aβ40 by its N-terminal or its RRM2 region (Fig. 15F).

3.2.2 ^{1}H-^{15}N Heteronuclear Single-Quantum Coherence nuclear magnetic resonance of protein (^{1}H-^{15}N HSQC protein NMR)

3.2.2.1 ^{15}N-Aβ40 in the presence and absence of TDP-43 variants

To ensure the ^{1}H-^{15}N HSQC NMR graph was the same for ^{15}N-Aβ40 prepared by myself and that from reference [36], the ^{1}H-^{15}N HSQC NMR experiments of ^{15}N-Aβ40 alone was performed first (Fig. 16A). The spectra showed dispersed signals that was similar to the reference and indicated ^{15}N-Aβ40 did not aggregate under the NMR

doi:10.6342/NTU201903526

conditions described in the first ^{15}N-Aβ40 preparation methods. The first promising candidate, TDP-43 N-term, was added into ^{15}N-Aβ40 on the concentration ten times higher than that of ^{15}N-Aβ40 in ThT assay (Fig. 16B, left panel). However, there was no significant chemical shift perturbation appeared, which indicated no obvious NMR signals movement on the NMR graph. Therefore, the concentration of TDP-43 (1-100) increased to 200 μM, which was 20 times higher than the concentration of ^{15}N-Aβ40 but no significant changes appeared (Fig. 16B, right panel), indicating no protein protein interaction between ^{15}N-Aβ40 and TDP-43 (1-100). The next promising candidate was TDP-43 (1-265) because it contained TDP-43 N-term and TDP-43 RRM1+2 domain, which were both the possible interaction site suggested by ThT assay. The condition was chosen based on the Octet experiments done by one of our lab members, which suggested equal molar ratio of biotin-Aβ40 could interact with TDP-43 (1-265) in the scale of nM. Despite the equal molar ratio, I tested multiple conditions, such as the suggested buffer condition of ^{15}N-Aβ40 and the buffer condition of Octet, which was pH 8.0 and unfortunately, the ^{1}H-^{15}N HSQC NMR graph was poor in pH 8.0 buffer (Fig. 16D). Furthermore, in pH 6.8 NMR buffer, I tested the temperature condition of ThT assay, which was 298K (25˚C), no significant chemical shift perturbation appeared in ^{1}H-^{15}N HSQC NMR graph (Fig. 16E). After all these tested conditions did not work out, I thought maybe TDP-43 (1-100) did not participate in interacting with ^{15}N-Aβ40. In this case, the part of TDP-43 (1-100) was not necessary. TDP-43 (101-265), containing the TDP-43 RRM1+2, was chosen as the third promising candidate (Fig. 16C down panel). Full-length TDP-43 was also tested but the concentration was low in the suggested condition, pH 6.8 (Fig. 16C, upper panel). Hence, I focused on TDP-43 (101-265), which could obtain high concentration and high

doi:10.6342/NTU201903526

concentration ratio was good for ^{1}H-^{15}N HSQC NMR testing. After the high concentration ratio was tested, the concentration of TDP-43 (101-265) was 20 times of the concentration of ^{15}N-Aβ40, no significant chemical shift perturbation or intensity changed appeared (Fig. 16C, right panel). This indicated that no truncated TDP-43 could interact with ^{15}N-Aβ40, at least ^{1}H-^{15}N HSQC NMR could not detect the interaction.

3.2.2.2 ^{15}N-TDP-43 (1-100) in the presence and absence of Aβ40

Although there was no chemical shift perturbation in ^{15}N-Aβ40 NMR graph, it was still worth trying to reversed the ^{15}N labeled protein from ^{15}N-Aβ40 to ^{15}N-TDP-43 (1-100) (Fig. 17). Aβ40 without ^{15}N labeled was added into ^{15}N-TDP-43 (1-100). The highest concentration ratio of Aβ40 to ^{15}N-TDP-43 (1-100) was 1.3 to 1 (Fig. 17A). When Aβ40 buffer was added into ^{15}N-TDP-43 (1-100) as a buffer control (Fig. 17B), it also caused chemical shift perturbation and the level and direction were the same as it contained Aβ40. This suggested that it was Aβ40 buffer that caused the chemical shift perturbation in ^{15}N-TDP-43 (1-100) NMR graph. In the Aβ40 preparation, GdnHCl was used to dissolve and monomerize Aβ40. According to the NMR results, the GdnHCl treatment to monomerize Aβ40 would affect the conformation of ^{15}N-TDP-43 (1-100)

In order to remove GdnHCl and to monomerize Aβ40, the Aβ40 preparation was changed to that used in ThT without DMSO because the concentration did not enhance after DMSO addition. The Aβ40 powder was dissolved directly in same NMR buffer as ^{15}N-TDP-43 (1-100) and the non-dissolved part was removed by centrifugation. The

doi:10.6342/NTU201903526

supernatant was added into ^{15}N-TDP-43 (1-100) (Fig. 18) and no significant difference appeared.

3.2.3 Enzyme-linked immunosorbent assay (ELISA)

Although up to the current tests, there were no significant changes appeared in ^{1}H-^{15}N HSQC protein NMR experiments, there were indications from ThT assays. Therefore, in order to find the binding site between Aβ40 and TDP-43, indirect ELISA was chosen, for it was a quick and straightforward methods.

TDP-43 was first coated on ELISA plate as an antigen and anti-TDP-43 antibody was used to block the possible binding site between Aβ40 and TDP-43. Biotin-Aβ40 was used to interact with TDP-43. If the binding site was not blocked by anti-TDP-43 antibodies, biotin-Aβ40 could interact with TDP-43 and SA-HRP could recognize biotin-Aβ40, which would lead to enhanced color formation. Because of the complicated protein components in this indirect ELISA assay, each component needed to optimize to best concentration. After a series of condition testing, I found the best antibody concentration was 2 nM because the intensity of anti-TDP-43 almost reached a plateau and had a significant difference from antibody control IgG2A (Fig. 19A). To contain non-specific binding caused by biotin-Aβ40 to anti-TDP-43 antibody, anti-TDP-43 antibodies were coated on ELISA plate and biotin-Aβ40 was added in serial dilution manner (Fig. 19B). The lowest concentration of biotin-Aβ40, which was 0.25 μM, had a lowest intensity that indicated low non-specific binding. Although the chosen concentration of biotin-Aβ40 in Fig. 19B seemed low, it could still bind to TDP-43 and obtain high intensity in Fig. 20A. Furthermore, when the concentration of biotin-Aβ40

doi:10.6342/NTU201903526

decreased, the intensity dropped dramatically, which suggested that 0.25 μM was the optimized concentration of biotin-Aβ40 in ELISA (Fig. 20B).

With the optimized concentration, different types of anti-TDP-43 antibodies were tested and refolded TDP-43 were coated in serial dilution manners in order to decrease TDP-43 binding site to biotin-Aβ40 (Fig. 21A). Although anti-TDP-43 (1-103) and anti-TDP-43 (205-222) antibodies did slightly decrease the intensity, TDP-O2, 6, 11 and anti-TDP-43 C-term had an obvious decrease in ELISA intensities, indicating they might block the binding site of TDP-43 and biotin-Aβ40. In order to reassure whether TDP-O2, 6, and 11 did block the binding site, the concentration of TDP-43 was adjusted to 5 μM, which based on hypothesis that one antibody bond two antigens by its two flexible regions. The intensity caused by TDP-O2, O6, and O11 addition was 0.5, which derive from non-specific binding of biotin-Aβ40 to blocking reagent, 2% BSA. Although biotin-Aβ40 would non-specifically bind to 2% BSA, the intensity of positive control, which was the interaction between biotin-Aβ40 and TDP-43 without anti-TDP-43 antibody interference, was much higher. This indicated that the interaction between TDP-43 and biotin-Aβ40 was real and that TDP-O2, O6, and O11 did interrupt the interaction between TDP-43 and biotin-Aβ40. (Fig. 21B).

Because of the background derived from biotin-Aβ40 and 2% BSA, the blocking reagent was substituted by 2.5% skim milk (Fig. 21C). Although the intensity of background became very low, the intensity of positive control dropped as well. When the concentration of anti-TDP-43 antibodies were the same as previous ELISA experiments, the trend was almost the same, suggesting TDP-43 (RRM1+2) and TDP-43 C-term were the main interaction site between TDP-43 and biotin-Aβ40. When the concentration of anti-TDP-43 antibodies decrease, the blocking effect was not so

doi:10.6342/NTU201903526

significant. However, TDP-O2 and anti-TDP-43 (205-222) antibodies still had a better blocking effect than other anti-TDP-43 antibodies, suggesting in the ELISA assay, biotin-Aβ40 preferred to interact with TDP-43 (RRM1+2) region.

doi:10.6342/NTU201903526

Chapter 4. Discussion

In the past few decades, Aβ40 cascade hypothesis was one of the main hypothesis to describe AD. In recent years, TDP-43 pathology started to gain people's attention and was recognized as the third pathological features in a subset of people living with Alzheimer's disease. However, the role of TDP-43 played in AD remain unknown. In a paper published by Dr. Yun-Ru Chen's lab, after incubation for 5 days, TDP-43 retained Aβ40 in oligomeric state rather than fibers. In a further research done by one of my lab members, Ting-Yu Chang, TDP-43 could interact with Aβ40 in nM level (data not published). Here, in ThT assay, I found that when the concentration of anti-TDP-43 antibody was the same as TDP-43, the lag phase of Aβ40 aggregation was earlier and the intensity was higher than Aβ40 alone. When incubating TDP-43 with low concentration of anti-TDP-43 (1-103) or anti-TDP-43 (205-222) for 3 hours and adding the mixture into Aβ40 solution, Aβ40 aggregation would be rescued to some degree after over 4 days of incubation. When the concentration of anti-human TDP-43 antibody increase to 0.05 μM, Aβ40 aggregation was completely rescued. It suggested that TDP-43 N-terminal and RRM2 domain might be the interaction site between Aβ40 and TDP-43 during long term incubation. Due to the complicated Aβ40 misfolding and aggregation process, it was unknown why the other anti-TDP-43 antibody alone, including TDP-O6 and TDP-O11 possessed the ability to inhibit Aβ40 from forming β-sheets completely. More experiments were needed to understand the reason.

In ^{1}H-^{15}N HSQC protein NMR experiments, in equal-molar ratio, no chemical shift perturbation appeared when Aβ40 was added into ^{15}N-TDP-43 (1-100) solution, suggesting that under this condition, Aβ40 did not interact with ^{15}N TDP-43 (1-100). Due to low concentration of Aβ40 in the NMR buffer, it was hard to increase the ratio

doi:10.6342/NTU201903526

of Aβ40 to ^{15}N-TDP-43 (1-100). In the reversed ^{15}N label NMR experiment, GdnHCl may affect TDP-43 conformation, leading to no interaction with ^{15}N-Aβ40. In the ELISA assay, anti-human TDP-43 antibody, which targeted TDP-43 C-term or TDP-43 RRM1+2 domain, showed significant intensity drop than other antibody did. It indicated that in a short incubation time, which was 2 hr, Aβ40 tend to interact with these two parts of TDP-43 while TDP-43 was coated on ELISA plate. Due to the short incubation time of ELISA assay, it could only provide the initial interaction pattern of Aβ40 and TDP-43. The long incubation time and β-sheet detection of ThT assay provided insights into how TDP-43 affect Aβ40 aggregation.

In protein NMR experiments, it focused on monomer form of protein-protein interaction because only monomer form of protein could provide a sparse NMR spectrum. That was the main difference to ThT assay and ELISA assay. In ThT assay and ELISA assay, full-length human TDP-43 was mostly in oligomer form. In addition, the interaction between human TDP-43 and Aβ40 might not follow the pattern of normal protein-protein interaction because Aβ40 was an intrinsic disorder protein. There was a paper suggested that one NMR experiments, paramagnetic relaxation enhancement experiments (PRE), could detect intrinsic disorder protein-protein interaction at low affinity, low population (0.5~5%), and short lifetime (250~500 μs) [37]. According to this paper, if the interaction between TDP-43 and Aβ40 was transient, I should use PRE experiments instead.

According to my results and Ting-Yu Chang's master thesis, TDP-43 N-term, which was reported to be responsible for TDP-43 dimerization, played an important role in affecting Aβ40 aggregation. When anti-TDP-43 (1-103) antibody interacted with it, TDP-43 lost the ability to inhibit Aβ40 aggregation (Fig. 15C). However, in ELISA

doi:10.6342/NTU201903526

assay, after anti-TDP-43 (1-103) interacted with TDP-43 N-term, the blocking effect was not obvious compared to other anti-TDP-43 antibodies (Fig. 21). In the biolayer interferometry assay, TDP-43 N-term could not interact with biotin-Aβ40. These data suggested that although TDP-43 N-term really played an important role in interfering Aβ40 aggregation, it could not interact with it. TDP-43 N-term may play a supportive character in inhibiting Aβ40 aggregation.

As for TDP-43 (RRM1+2) region, it could slightly affect Aβ40 aggregation in ThT assay. However, when anti-TDP-43 (205-222) was applied, TDP-43 lost the ability to influence Aβ40 aggregation (Fig. 15C). In biolayer interferometry assay, it had a strong binding affinity to biotin-Aβ40 and in ELISA assay, when TDP-O2 and TDP-O11 were applied, biotin-Aβ40 could not bind to TDP-43 (Fig. 21), suggesting that TDP-43 (RRM1+2) was the binding site between Aβ40 and TDP-43. In ELISA assay, it pointed out that TDP-43 C-term also played a role in interacting with biotin-Aβ40. In summary, TDP-43 used its RRM1+2 region to interact with Aβ40 and its N-term to support the inhibition of Aβ40 aggregation.

There are several technical improvements in ^{1}H-^{15}N HSQC protein NMR experiments and in ELISA assay. For Aβ40 treatment, despite using HFIP to monomerize Aβ40, NaOH is also widely used to monomerize Aβ40 and it may obtain Aβ40 fibrils more readily [38]. Particularly in NMR experiments, there are several labs that use NaOH to treat ^{15}N-Aβ40 and perform ^{1}H-^{15}N HSQC protein NMR experiments [36, 39, 40]. In addition to different Aβ40 treatment, the pH value of NMR buffer used to dissolve ^{15}N Aβ40 was above pH 7.0, indicating higher pH value could obtain higher concentration of Aβ40, which would benefit NMR experiments. On the other hand, ^{15}N TDP-43 (1-100) purified by myself could not 100% resemble the NMR signals

doi:10.6342/NTU201903526

assignments in the published paper [21] in similar buffer (data not shown). Therefore, ^{15}N-TDP-43 (1-80) might be a promising candidate because it had dispersed NMR signals in pH 7.4, phosphate buffer [41]. The pH value of the buffer also could obtain high concentration of Aβ40 [36], which could test more NMR conditions.

As for ELISA assay, although 2% BSA was commonly used as a blocking reagent, it was reported to inhibit Aβ40 aggregation when the concentration of BSA was the same or higher than Aβ40 [42]. It proposed that BSA capped the hydrophobic sites on Aβ40, which block the monomer addition to Aβ40 and inhibit Aβ40 aggregation. In my study, the concentration of 2% BSA, which was 300 μM of BSA, was around 1,000-fold higher than biotin-Aβ40, indicating that BSA might compete with TDP-43 for interacting with biotin-Aβ40. Indeed, in the absence of TDP-43, it had a strong background value of 0.5, showing BSA might interact with biotin-Aβ40. However, in the presence of TDP-43, it had an even stronger intensity, indicating that biotin-Aβ40 preferentially bond to TDP-43 not BSA. In order to eliminate the interaction between blocking reagents and biotin-Aβ40, I chose 2.5% skim milk as a new blocking reagent. Although the background intensity dropped below 0.1, the intensity of positive control dropped to 0.4 as well (Fig. 21C). To increase the intensity of positive control, the concentration of biotin-Aβ40 and TDP-43 needed to increase.

In ThT assay, when the concentration of anti-TDP-43 antibody increased to 0.05 μM, they didn't significantly affect the lag phase of Aβ40 aggregation (Fig. 15D). Therefore, under this concentration, TDP-O2, O6, O11, and O9 could apply to TDP-43 again in order to compare their ELISA results to ThT assay results and obtain a more comprehensive view of the anti-TDP-43 antibodies effect on TDP-43 and Aβ40.

doi:10.6342/NTU201903526

Figures

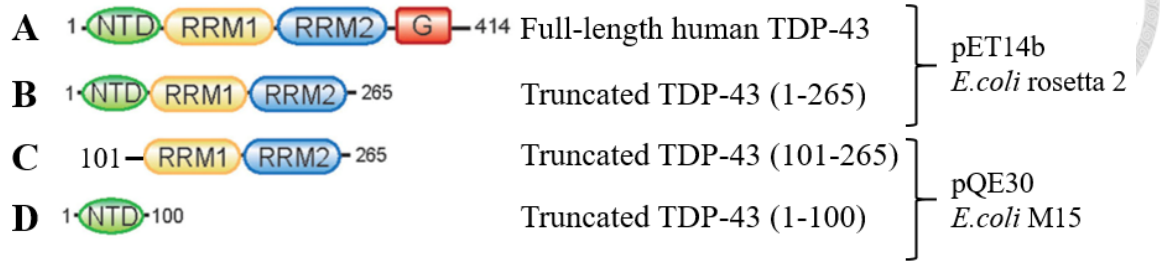

Figure 1. Structural illustration of human full-length and truncated TDP-43. Full-length TDP-43 contained a N-terminal domain, two RNA recognition domains, and a glycine rich region. Various constructs of TDP-43 were listed and their corresponding expression vectors and expression host were labeled on the right of each construct.

Figure 2. The sequence alignment of human and mouse full-length TDP-43. The sequence alignment was done by Uniprot Protein Information Resource. TDP-43 from two species had 96.1% identity. The differences were highlighted by black square.

doi:10.6342/NTU201903526

A

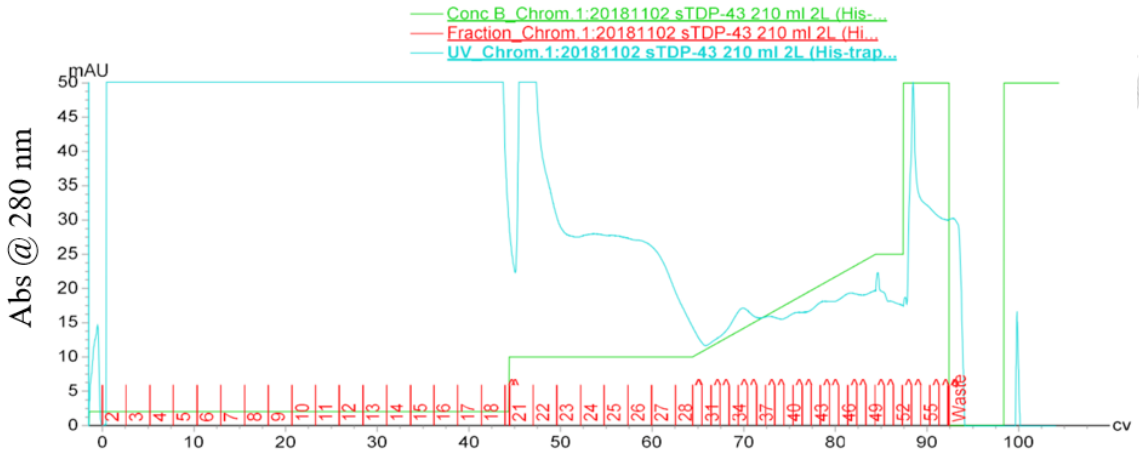

B

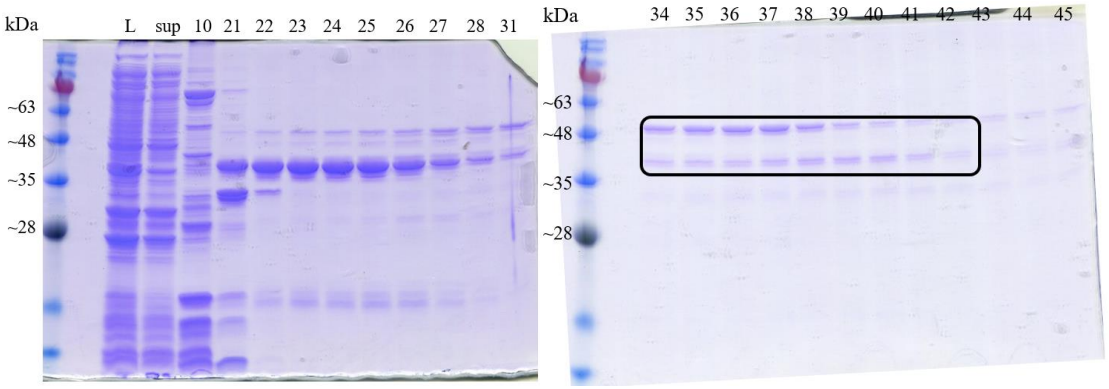

Figure 3. Expression of full-length TDP-43 by IPTG induction at O.D.600=0.6. (A) FPLC chromatogram of full-length TDP-43 purification. The UV 280 nm was presented in Y axis and the column volume was in X axis. (B) Tris-glycine SDS-PAGE with FPLC fractions.

doi:10.6342/NTU201903526

A

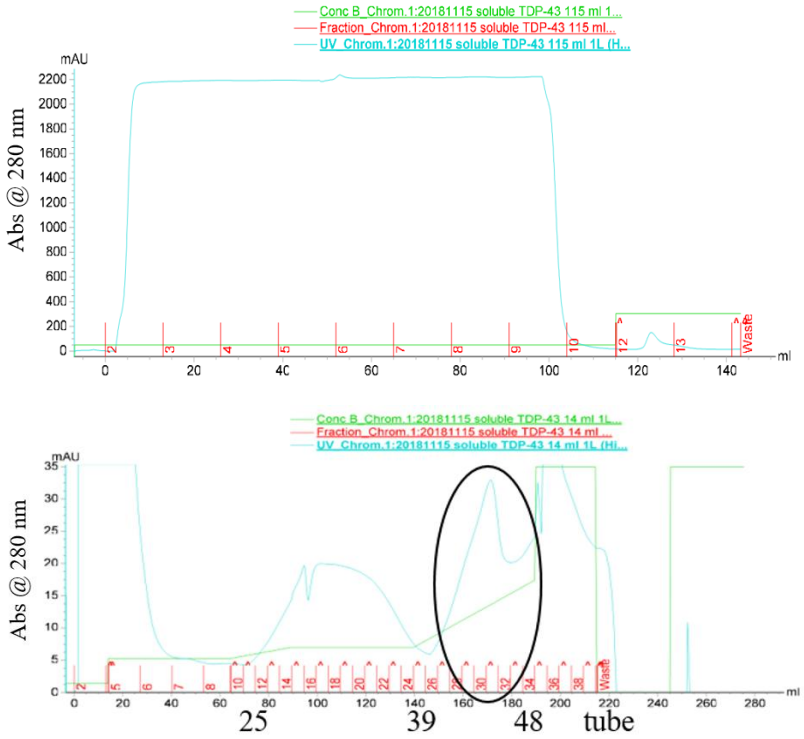

B

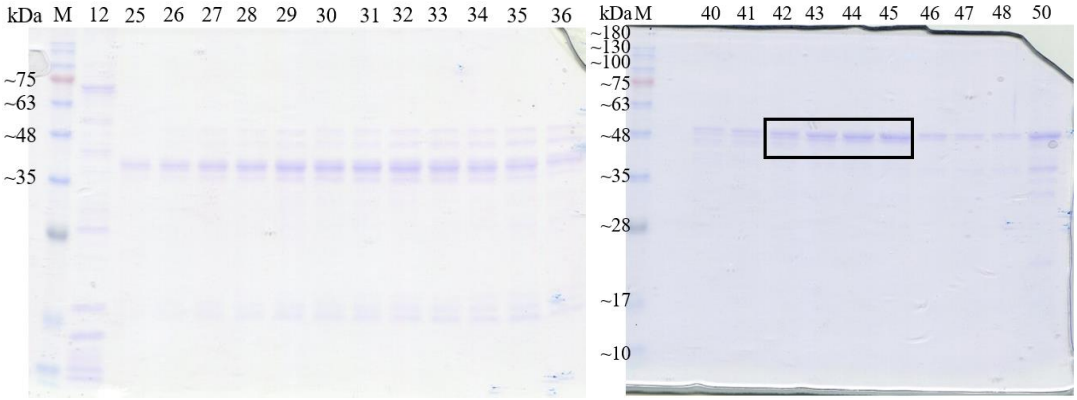

Figure 4. Purification of full-length soluble TDP-43. (A) FPLC chromatogram of full-length TDP-43 in pET14b from *E.coli* rosetta 2. The UV 280 nm was presented in Y axis and the elution volume was in X axis. (B) SDS-PAGE of the washing and elution fractions.

doi:10.6342/NTU201903526

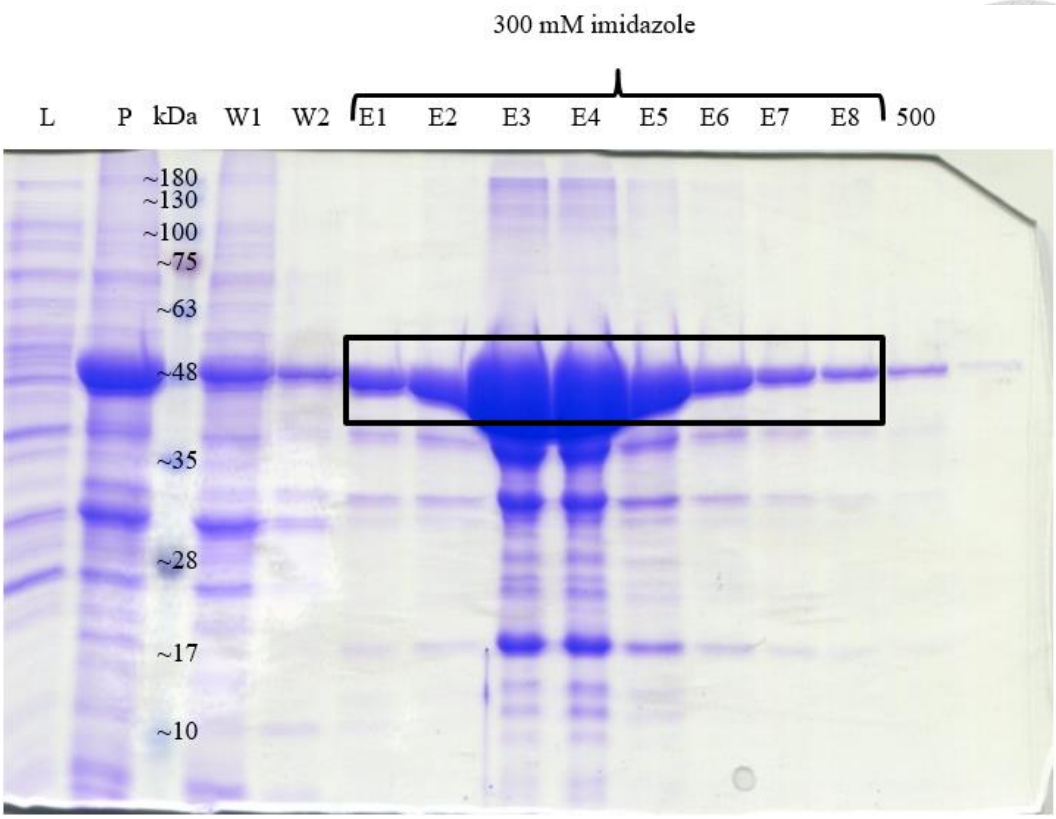

Figure 5. Purification of insoluble full-length TDP-43 by open column. Fractions from each step of the purification was checked by 13% Tris-glycine SDS-PAGE.

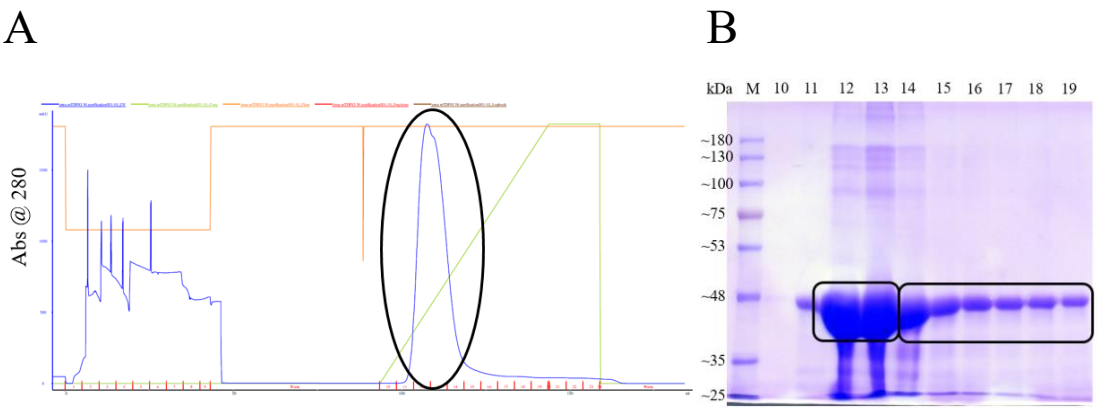

Figure 6. Purification of insoluble mouse full-length TDP-43 by Ni-NTA column. (A) FPLC chromatogram of full-length mouse TDP-43 in pQE80 from *E.coli* M15. The UV 280 nm was presented in Y axis and the column volume was in X axis. (B) SDS-PAGE of the elution fractions.

doi:10.6342/NTU201903526

A

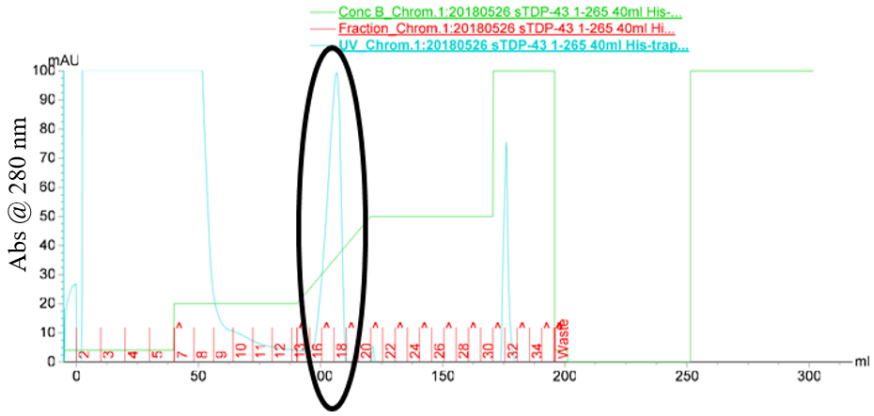

B

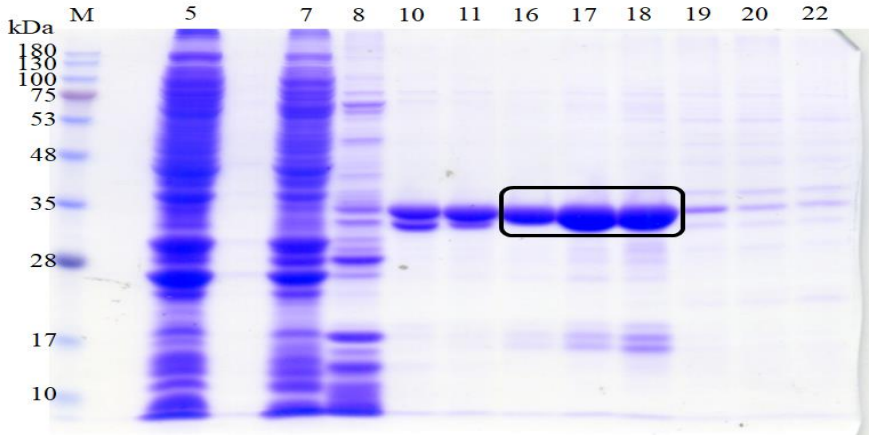

Figure 7. Purification of soluble truncated human TDP-43 (1-265). (A) FPLC chromatogram of truncated human TDP-43 (1-265) in pET14b from *E.coli* rosetta 2. The UV 280 nm was presented in Y axis and the elution volume was in X axis. (B) SDS-PAGE of the washing and elution fractions.

doi:10.6342/NTU201903526

A

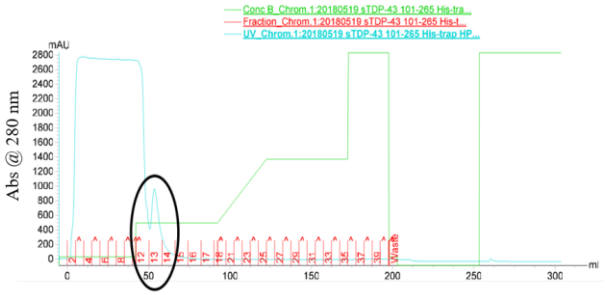

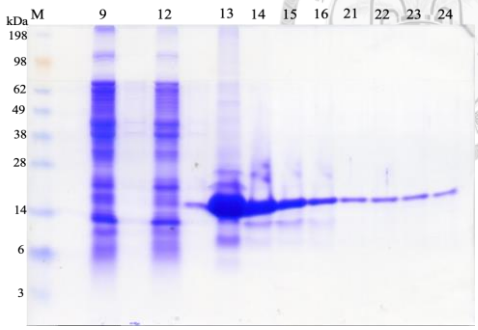

B

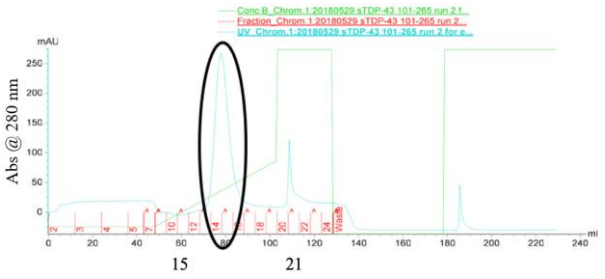

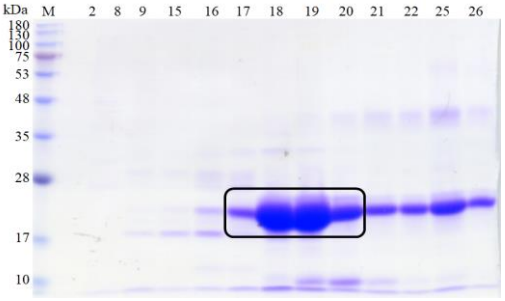

Figure 8. Purification of soluble truncated human TDP-43 (101-265). (A, left panel) FPLC chromatogram of truncated human TDP-43 (101-265) in pQE30 from *E.coli* M15. The UV 280 nm was presented in Y axis and the elution volume was in X axis. (A, right panel) SDS-PAGE of the washing and elution fractions. (B, left panel) FPLC chromatogram of truncated human TDP-43 (101-265) diluted to 50 ml from (A, fraction 13). The UV 280 nm was presented in Y axis and the elution volume was in X axis. (B, right panel) SDS-PAGE of the washing and elution fractions.

doi:10.6342/NTU201903526

A

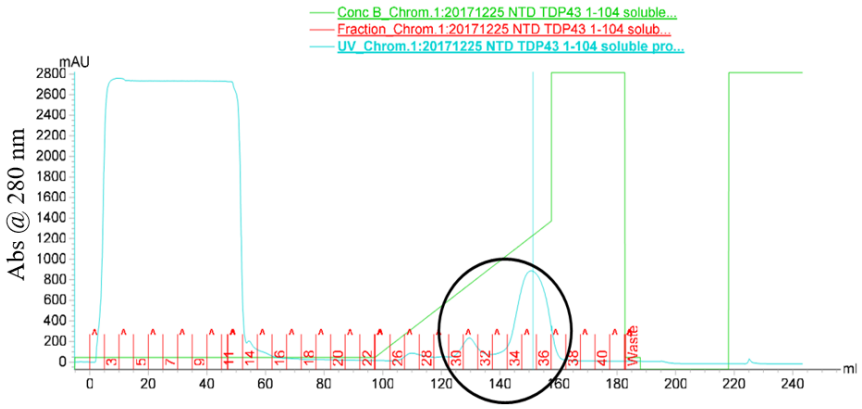

B

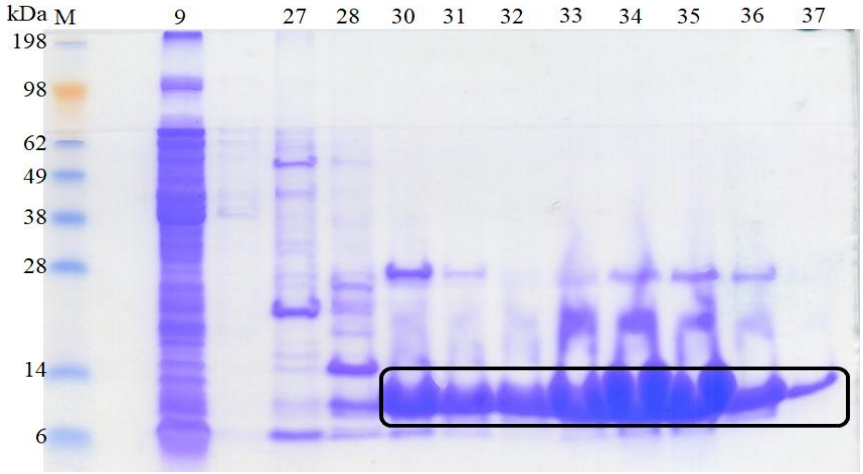

Figure 9. Purification of soluble truncated human TDP-43 (1-100). (A) FPLC chromatogram of truncated human TDP-43 (1-100) in pQE30 from *E.coli* M15. The UV 280 nm was presented in Y axis and the elution volume was in X axis. (B) SDS-PAGE of the washing and elution fractions.

doi:10.6342/NTU201903526

A

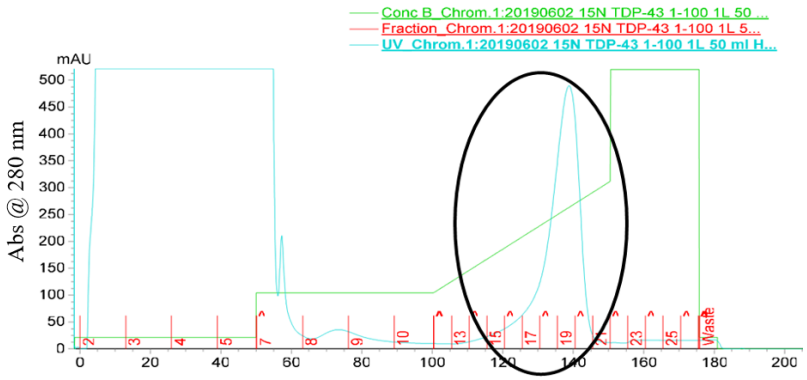

B

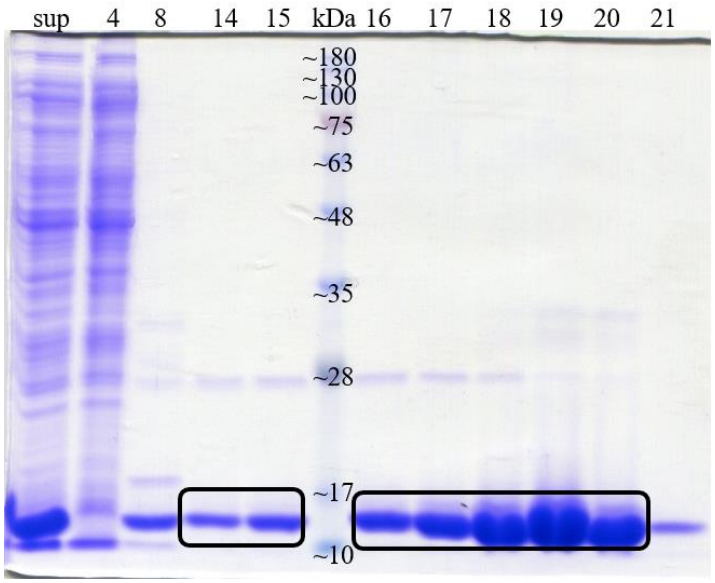

Figure 10. Purification of 15N labeled soluble truncated-human TDP-43 (1-100). (A) FPLC chromatogram of ^{15}N labeled truncated human TDP-43 (1-100) in pQE30 from *E.coli* M15. The UV 280 nm was presented in Y axis and the elution volume was in X axis. (B) SDS-PAGE of the washing and elution fractions.

doi:10.6342/NTU201903526

A

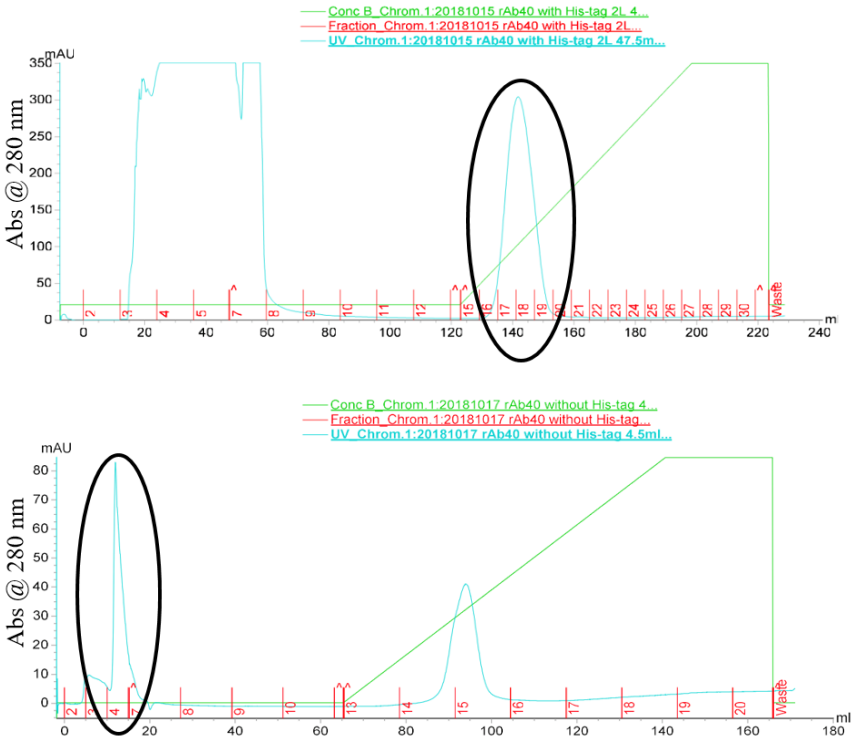

B

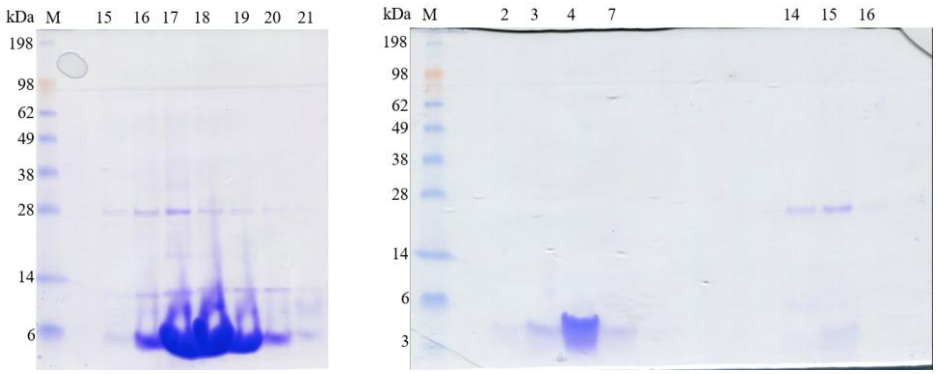

Figure 11. Purification of Aβ40 without His-tag. (A) FPLC chromatogram of His-Aβ40 from *E.coli* BL21 DE3*. The UV 280 nm was presented in Y axis and the elution volume was in X axis. (B) SDS-PAGE of the elution fractions. The His-tag of Aβ40 was proteolyzed by TEV protease and Aβ40 without His-tag was purified again.

doi:10.6342/NTU201903526

C

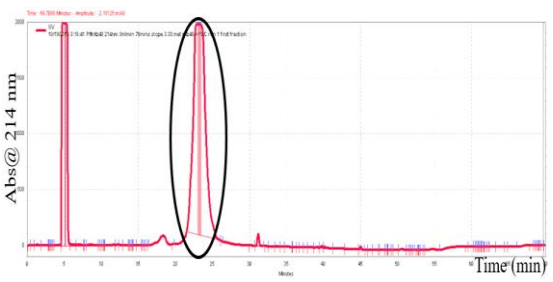

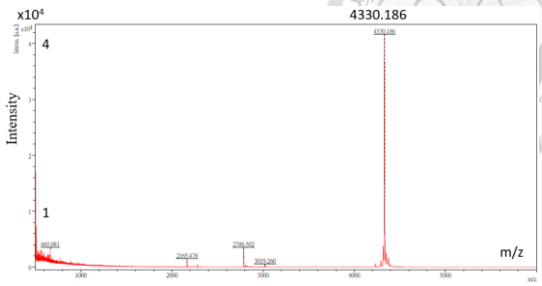

D

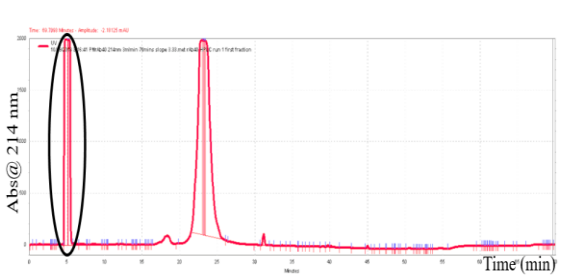

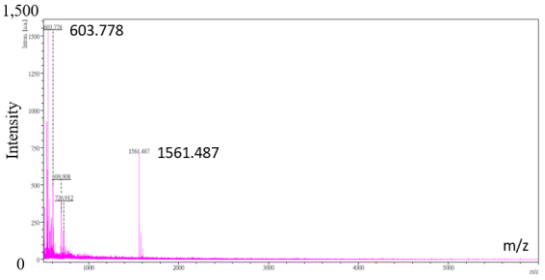

Figure 11. Purification of Aβ40 without His-tag. (C) The second peak in the HPLC chromatogram was checked by MALDI-TOF/TOF and the m/z value was similar to Aβ40 theoretical m/z value, which was 4330. (D) The first peak in the HPLC chromatogram was also checked by MALDI-TOF/TOF and Aβ40 theoretical m/z value did not appear.

doi:10.6342/NTU201903526

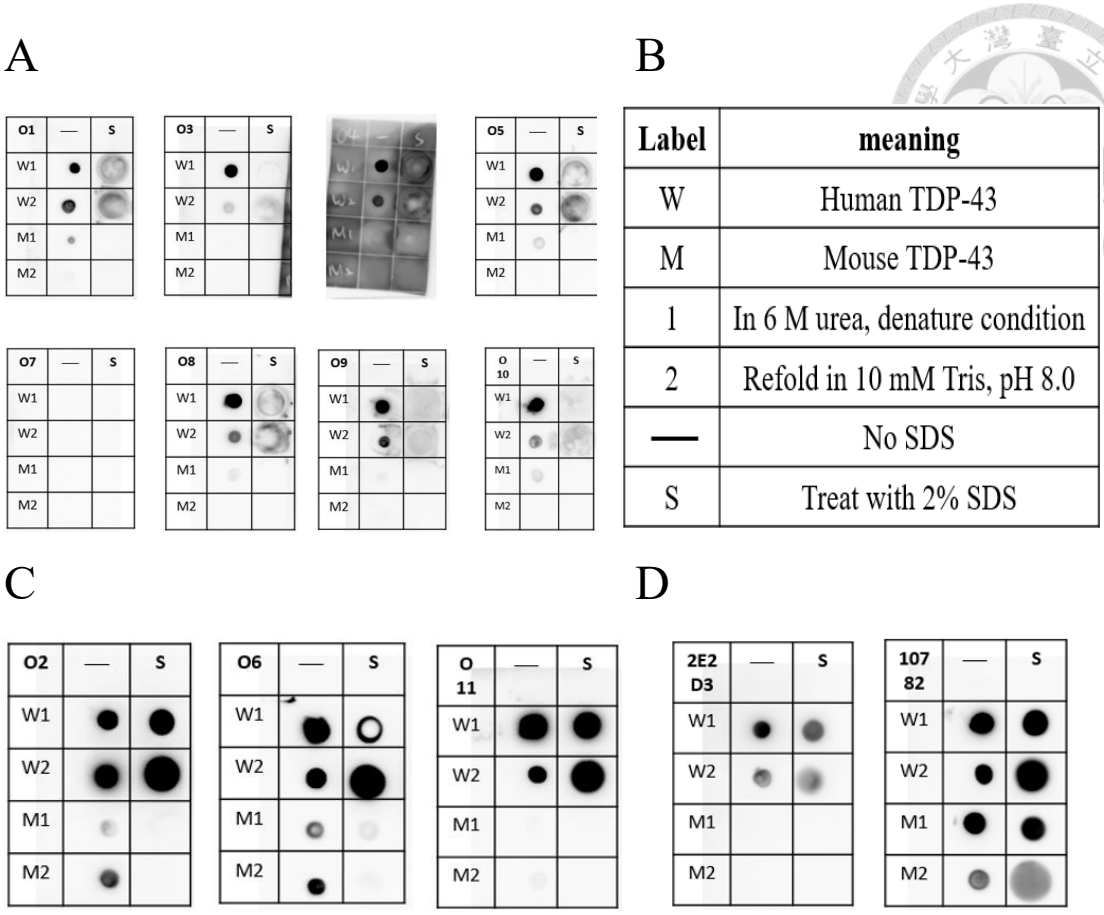

Label	meaning
W	Human TDP-43
M	Mouse TDP-43
1	In 6 M urea, denature condition
2	Refold in 10 mM Tris, pH 8.0
—	No SDS
S	Treat with 2% SDS

Figure 12. Characterization of monoclonal anti TDP-43 antibodies, TDP-O1 to O11 in short, by different types of human and mouse full-length TDP-43. Human and mouse TDP-43 were treated in different conditions and the details were in (B). All proteins were diluted to same concentrations, 4 μM and all TDP-O antibodies were used in 1 : 1,000 ratio, which might be over-saturated concentration. Monoclonal anti TDP-43 2E2D3 and polyclonal anti TDP-43 10782 antibodies recognized 205-222 and 1-260 respectively. (A) and (C) All TDP-O antibodies except TDP-O7 could recognize human TDP-43 when 2% SDS was not added. TDP-O1, O2, O5, O6, O8, and O10 might recognize mouse TDP-43 in denature condition. (D) Commercial monoclonal anti TDP-43 antibody, 2E2D3, and polyclonal anti TDP-43 antibody were used as positive controls.

doi:10.6342/NTU201903526

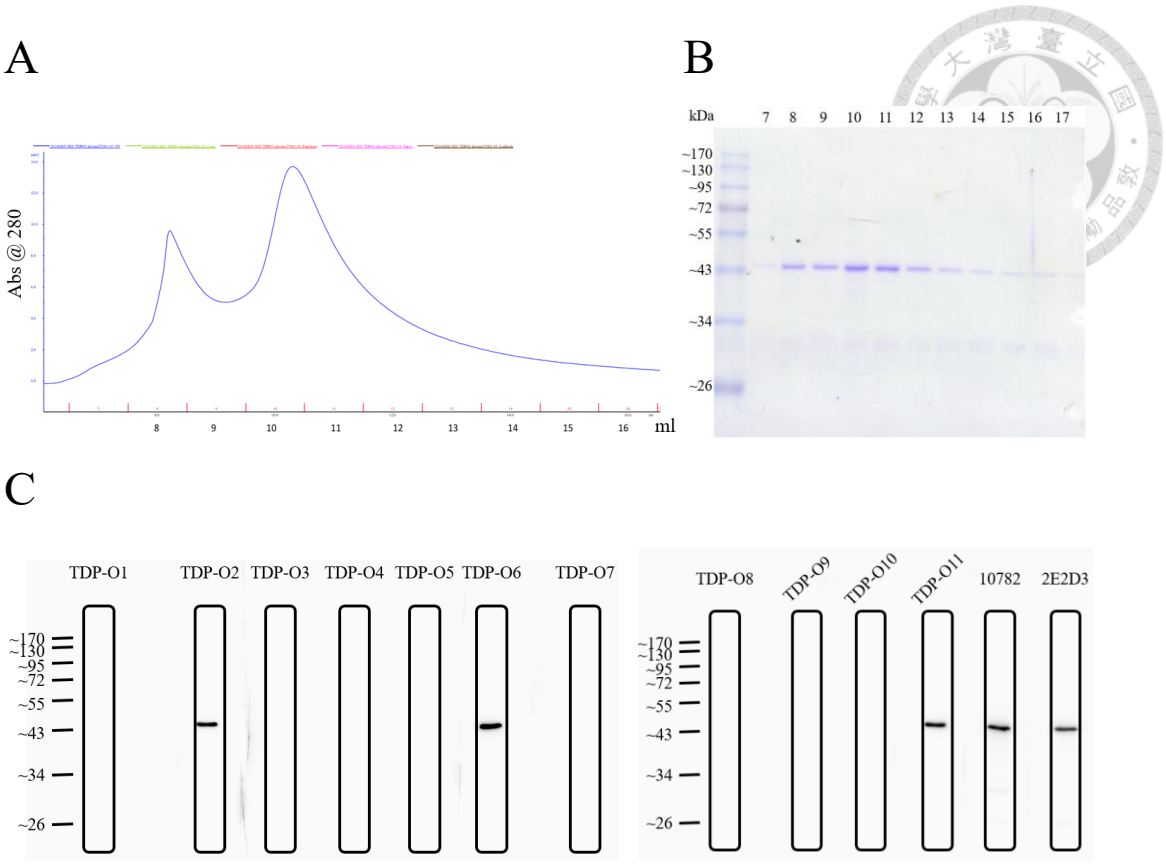

Figure 13. Monoclonal anti TDP-43 antibodies, TDP-O1 to O11, characterization by human TDP-43 monomer obtained from size exclusion. (A) FPLC size exclusion chromatogram. The UV 280 nm was presented in Y axis and the elution volume was in X axis. (B) SDS-PAGE of each fraction. (C) Western blot was used to characterize TDP-O antibody by using human TDP-43 monomer obtained from size exclusion fraction 15.

doi:10.6342/NTU201903526

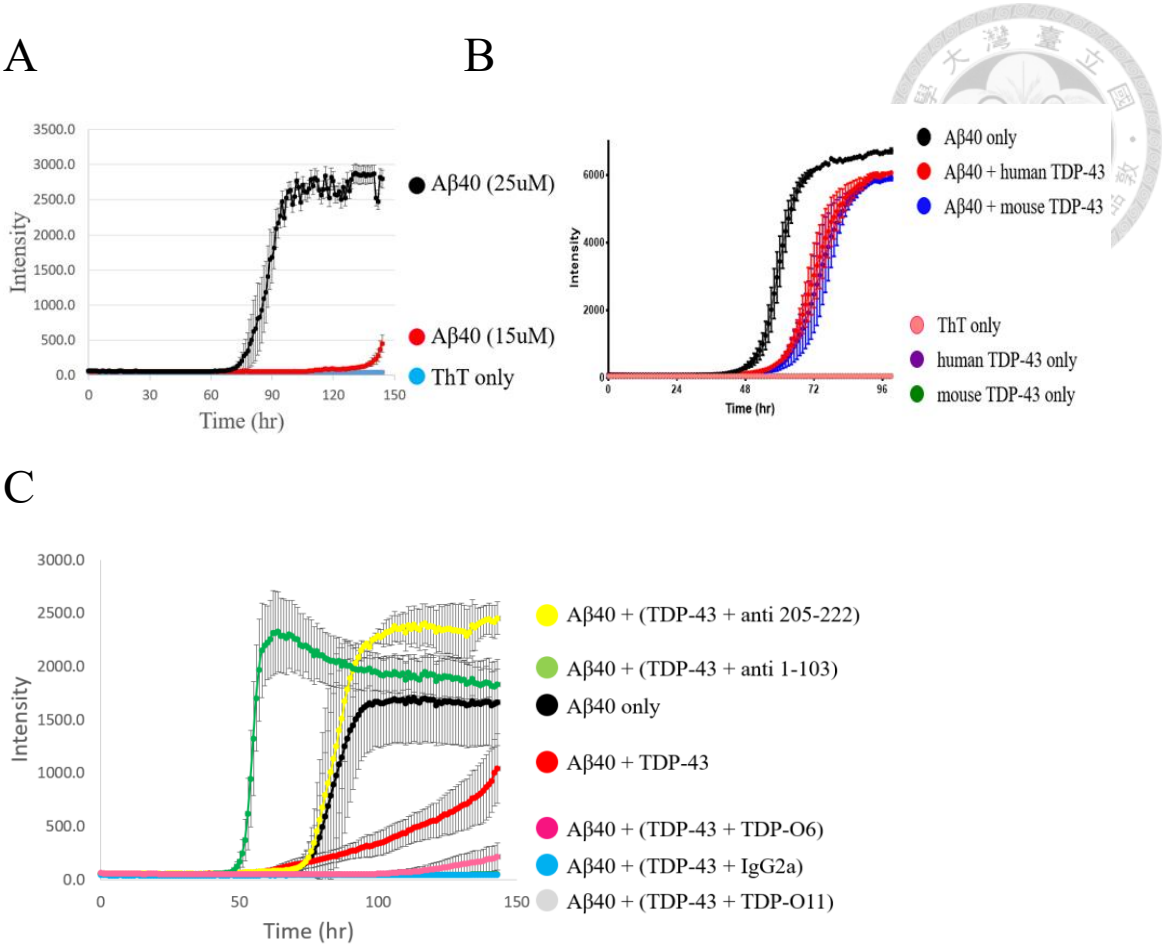

Figure 14. ThT assay to test the concentration of Aβ40 and anti TDP-43 antibodies and mouse TDP-43 effect on Aβ40 aggregation. (A) Test ThT assay for Aβ40 at 25 and 15 μM. (B) ThT assay for Aβ40 (25 μM) with and without human and mouse TDP-43 (0.25 μM). (C) ThT assay for Aβ40 with TDP-43 and anti-TDP-43 antibody complex. TDP-O6 and TDP-O11 recognized TDP-43 C-term and RRM1+2 domain respectively. Anti-TDP-43 (1-103) and anti-TDP-43 (205-222) recognize TDP-43 N-term and TDP-43 RRM2 domain respectively. The antibodies were incubated in equal-molar ratio with TDP-43 first for 3 hours. Then, the complex was added into Aβ40 solution containing 5 μM ThT.

doi:10.6342/NTU201903526

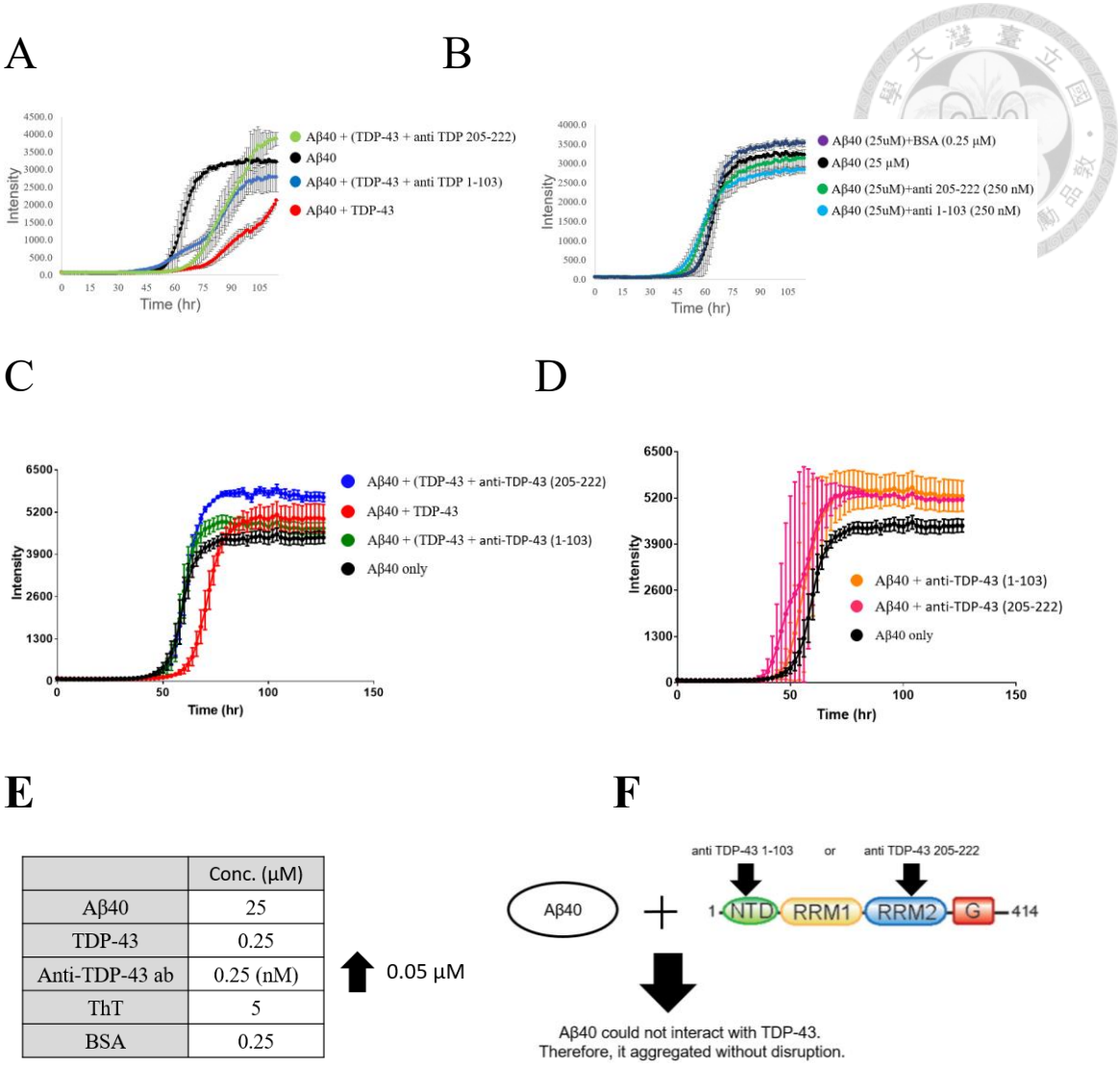

	Conc. (μM)
Aβ40	25
TDP-43	0.25
Anti-TDP-43 ab	0.25 (nM)
ThT	5
BSA	0.25

0.05 μM

Figure 15. ThT assay to investigate the interaction between Aβ40 and TDP-43. In ThT assay, Aβ40 concentration was 25 μM, full-length human TDP-43 was 0.25 μM, anti-TDP-43 antibody was 0.25 nM, and Thioflavin-T was 5 μM in (A, B). The concentration of anti-TDP-43 antibody was 0.05 μM in (C, D). The concentration was plot in chart in (E) and the conclusion was illustrated in (F).

doi:10.6342/NTU201903526

A

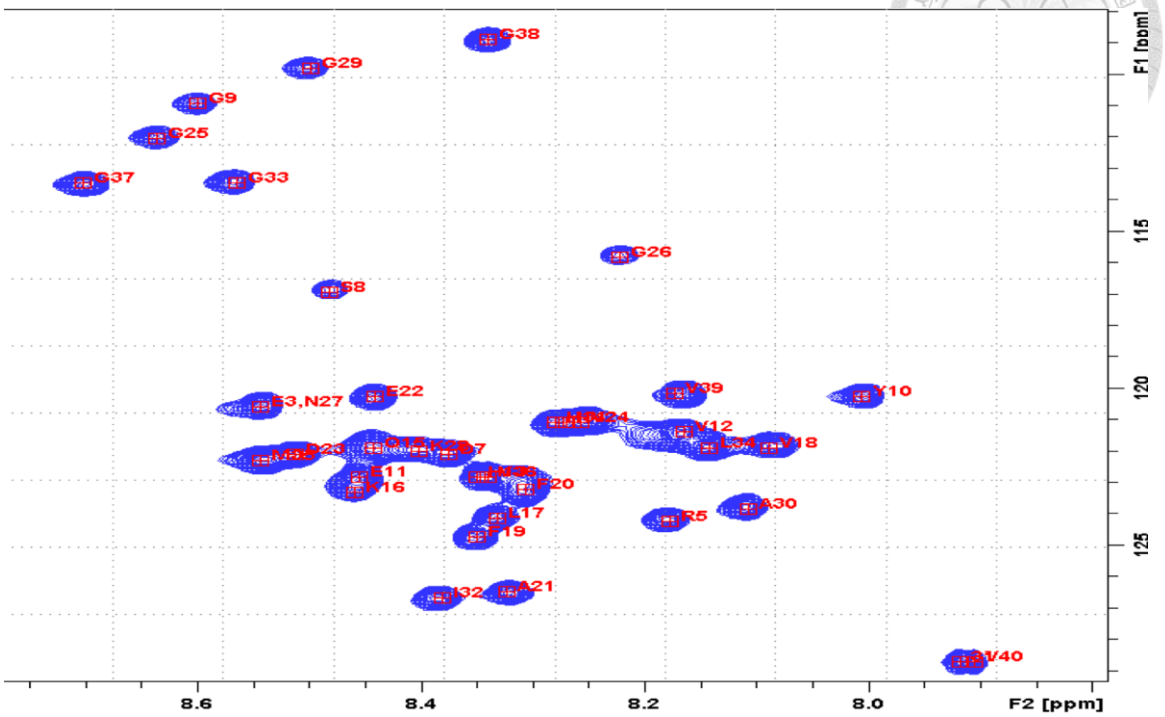

B

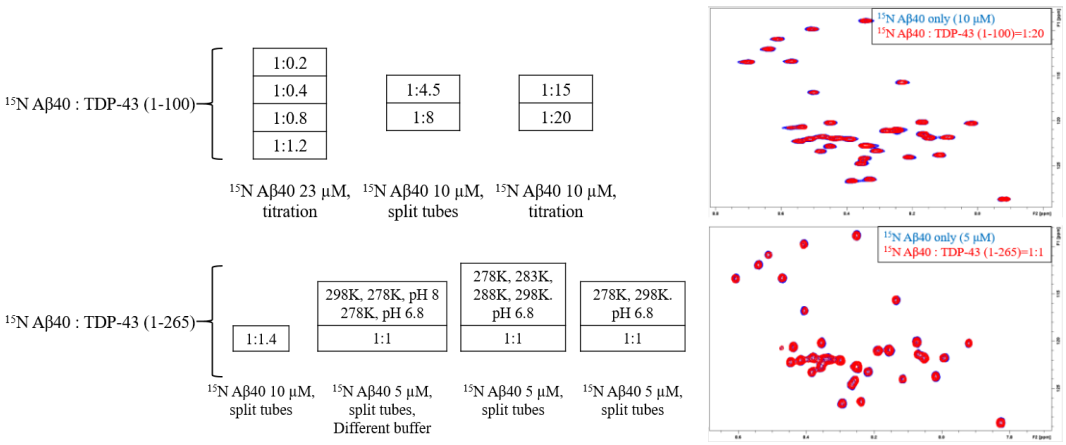

Figure 16. Using ^{1}H-^{15}N HSQC NMR with the addition of TDP-43 variants into ^{15}N Aβ40.

doi:10.6342/NTU201903526

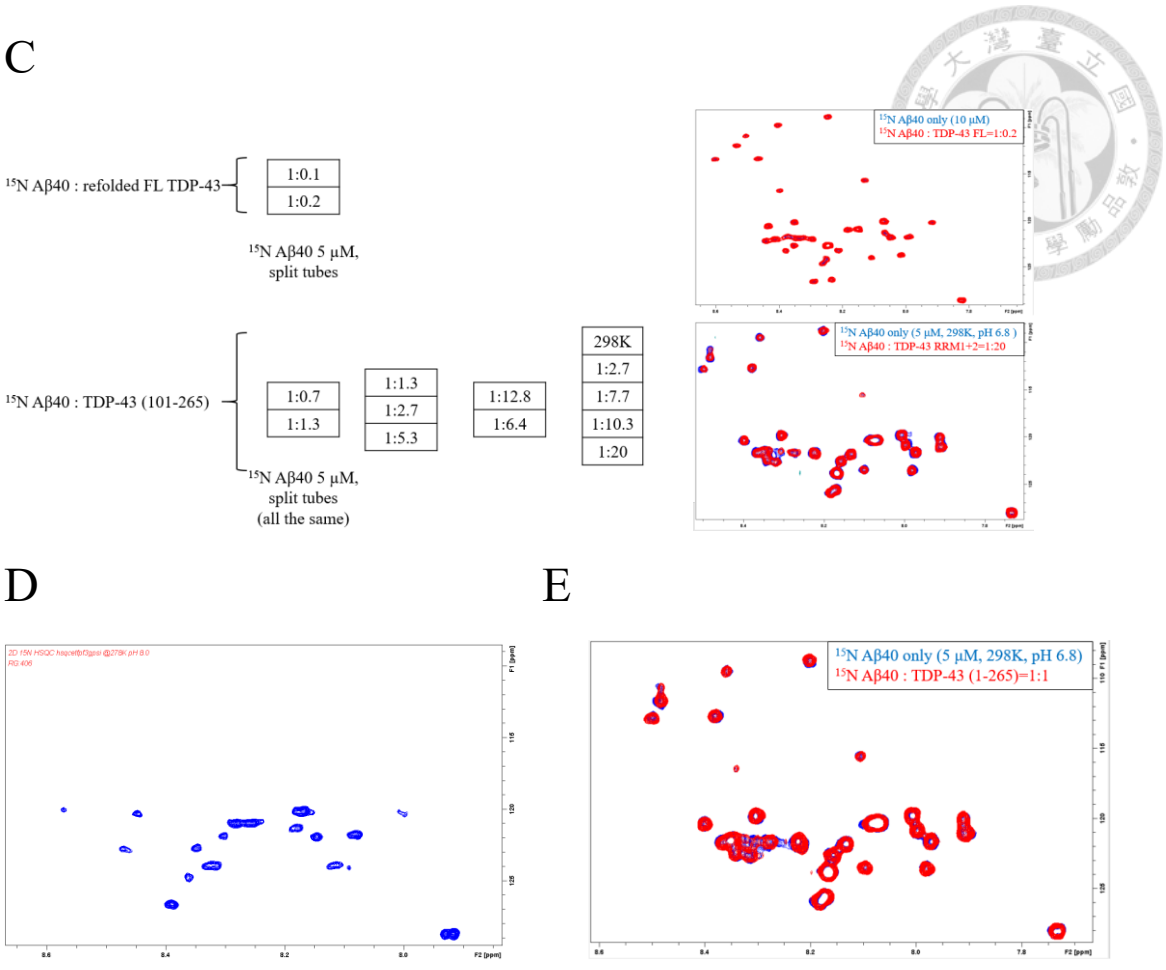

Figure 16. Using ^{1}H-^{15}N HSQC NMR with the addition of TDP-43 variants into ^{15}N Aβ40. (A) ^{1}H-^{15}N HSQC NMR graph of ^{15}N Aβ40 with signal assignments. (B, C) Different concentration of ^{15}N Aβ40 was used in these NMR experiments. Full-length human TDP-43 or truncated forms were added into ^{15}N Aβ40. The highest concentration ratio of ^{15}N Aβ40 and TDP-43 variants used were shown in the right panel. (D) ^{1}H-^{15}N HSQC NMR graph of ^{15}N Aβ40 in pH 8.0 buffer, containing 20 mM Tris, 50 mM NaCl at 278 K. (E) ^{1}H-^{15}N HSQC NMR graph contained ^{15}N Aβ40 in pH 6.8 buffer, containing 50 mM Tris, 20 mM NaCl at 298 K and equal-molar concentration of TDP-43 (1-265).

doi:10.6342/NTU201903526

A

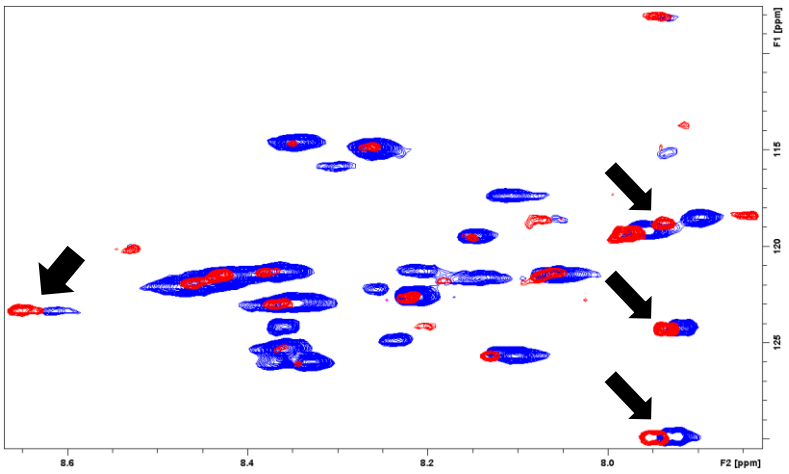

B

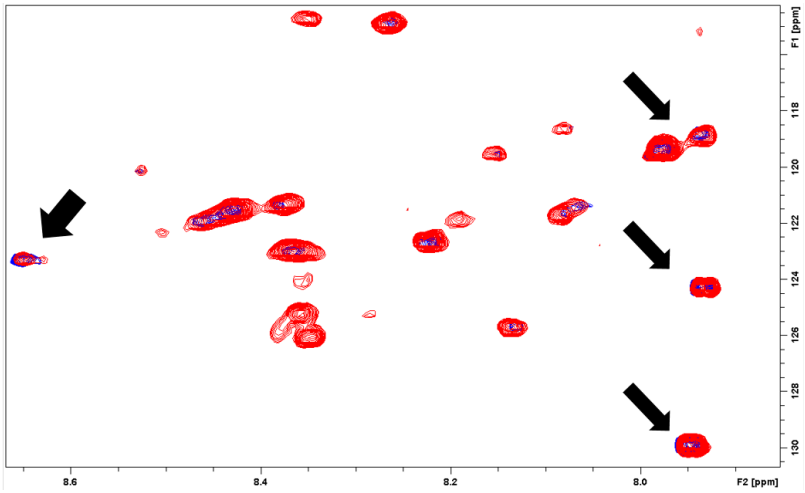

Figure 17. Fake chemical shift perturbation from GdnHCl effect on ^{15}N TDP-43 (1-100). (A) Aβ40 was first dissolved by 5 µl 8M GdnHCl and refolded in 95 µl NMR buffer. The refolded Aβ40 was quantified by BCA assay and added into ^{15}N TDP-43 (1-100) with 200 mM GdnHCl remaining. The significant chemical shift perturbation appeared after Aβ40 addition. ^{15}N TDP-43 (1-100) only was in blue and Aβ40 addition into ^{15}N TDP-43 (1-100) was in red.

doi:10.6342/NTU201903526

Figure 17. Fake chemical shift perturbation from GdnHCl effect on ^{15}N TDP-43 (1-100). (B) To check the buffer control, the NMR buffer with GdnHCl was added into ^{15}N TDP-43 (1-100) and the chemical shift perturbation appeared in the same way when Aβ40 was in it, indicating that the chemical shift difference was caused by GdnHCl. Aβ40 addition into ^{15}N TDP-43 (1-100) was in blue and NMR buffer contained GdnHCl addition into ^{15}N TDP-43 (1-100) was in red.

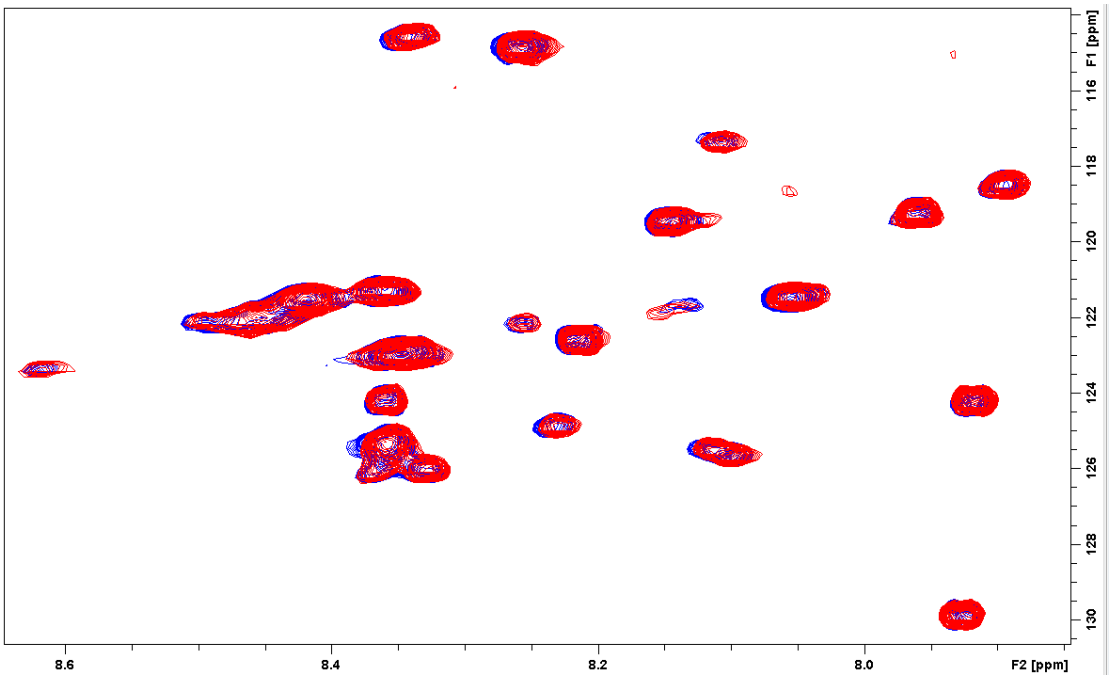

Figure 18. No chemical shift perturbation appeared after Aβ40 preparation change. The monomerization of Aβ40 was achieved by HFIP treatment and the solution was froze dry overnight to obtain powder form of Aβ40. The powder of Aβ40 was directly dissolved in NMR buffer and quantified by BCA assay after centrifugation to remove non-dissolve powder. The ^{15}N TDP-43 (1-100) only was blue and ^{15}N TDP-43 (1-100) with Aβ40 addition in 1:1.3 ratio was in red.

doi:10.6342/NTU201903526

A

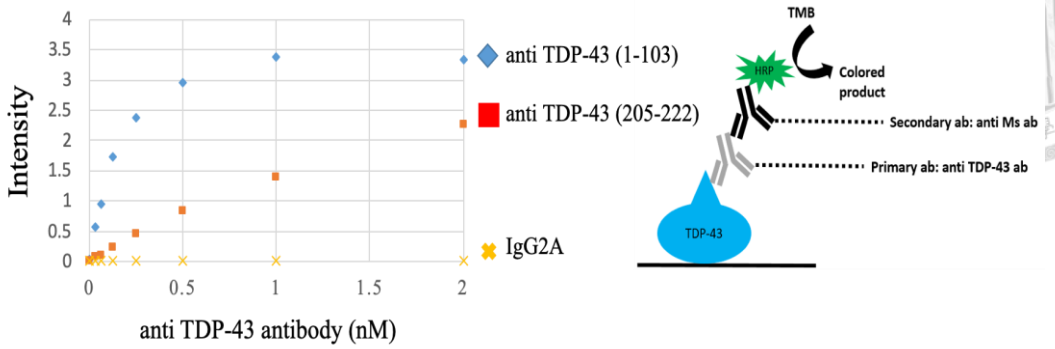

B

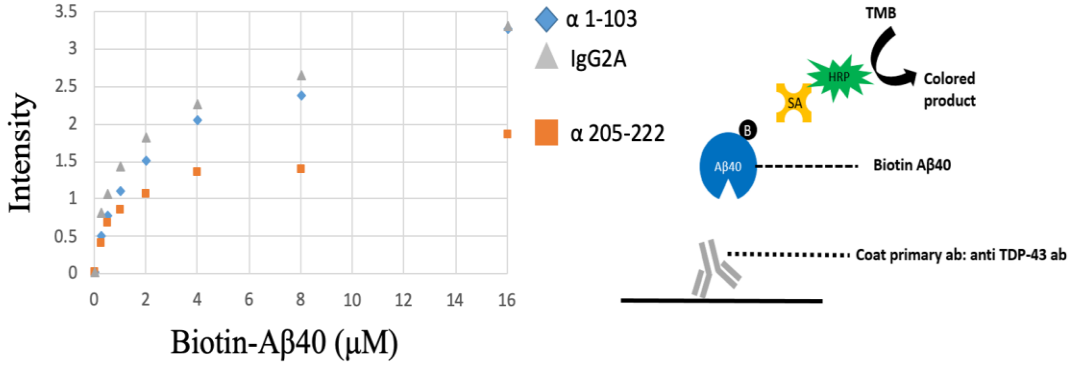

Figure 19. To find the working condition for TDP-43 and anti TDP-43 antibody in ELISA. (A) Refolded TDP-43 was coated on ELISA plate in 10 mM Tris, pH 8. Different concentration of anti TDP-43 antibodies was used to test the best concentration. (B) Anti TPD-43 antibodies were coated on ELISA plate in 10 mM Tris, pH 8. Biotin-Aβ40 was added into it to check the non-specific binding effect.

doi:10.6342/NTU201903526

A

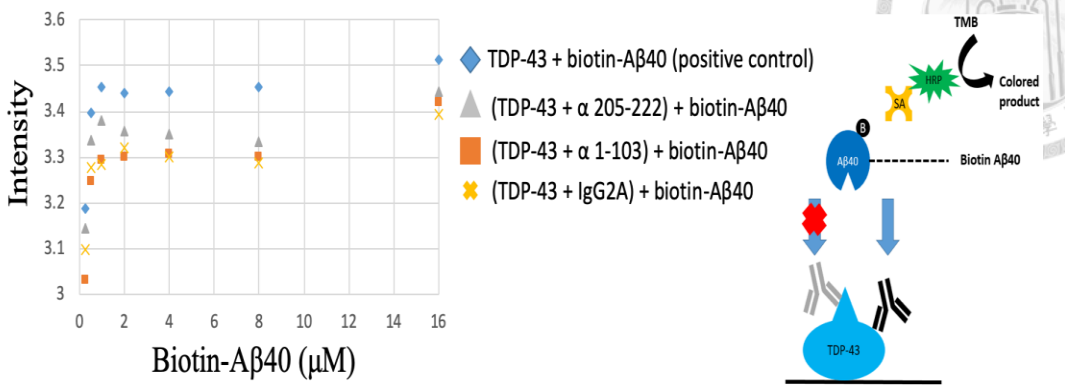

B

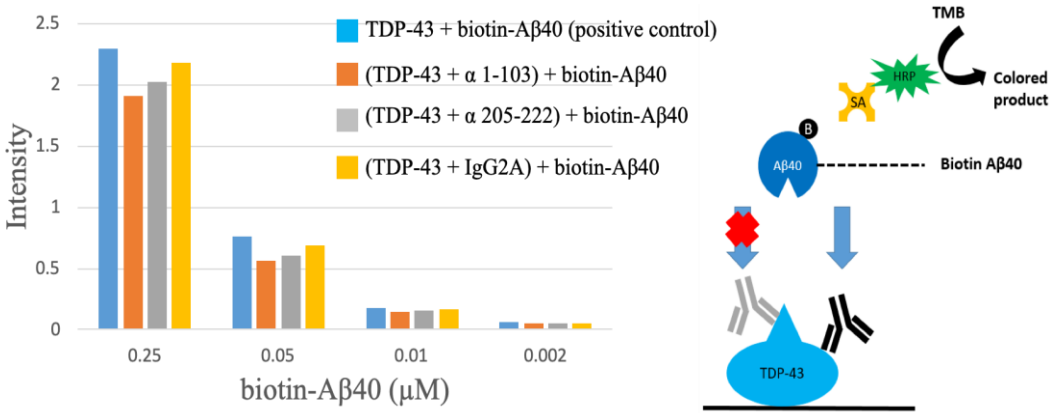

Figure 20. To find the working condition for anti TDP-43 antibody to disrupt TDP-43 and Aβ40 interaction. (A) Anti-TDP-43 antibody was used to block the binding site between Aβ40 and TDP-43. (B) To find the best biotin-Aβ40 concentration, lower biotin-Aβ40 concentration was applied.

doi:10.6342/NTU201903526

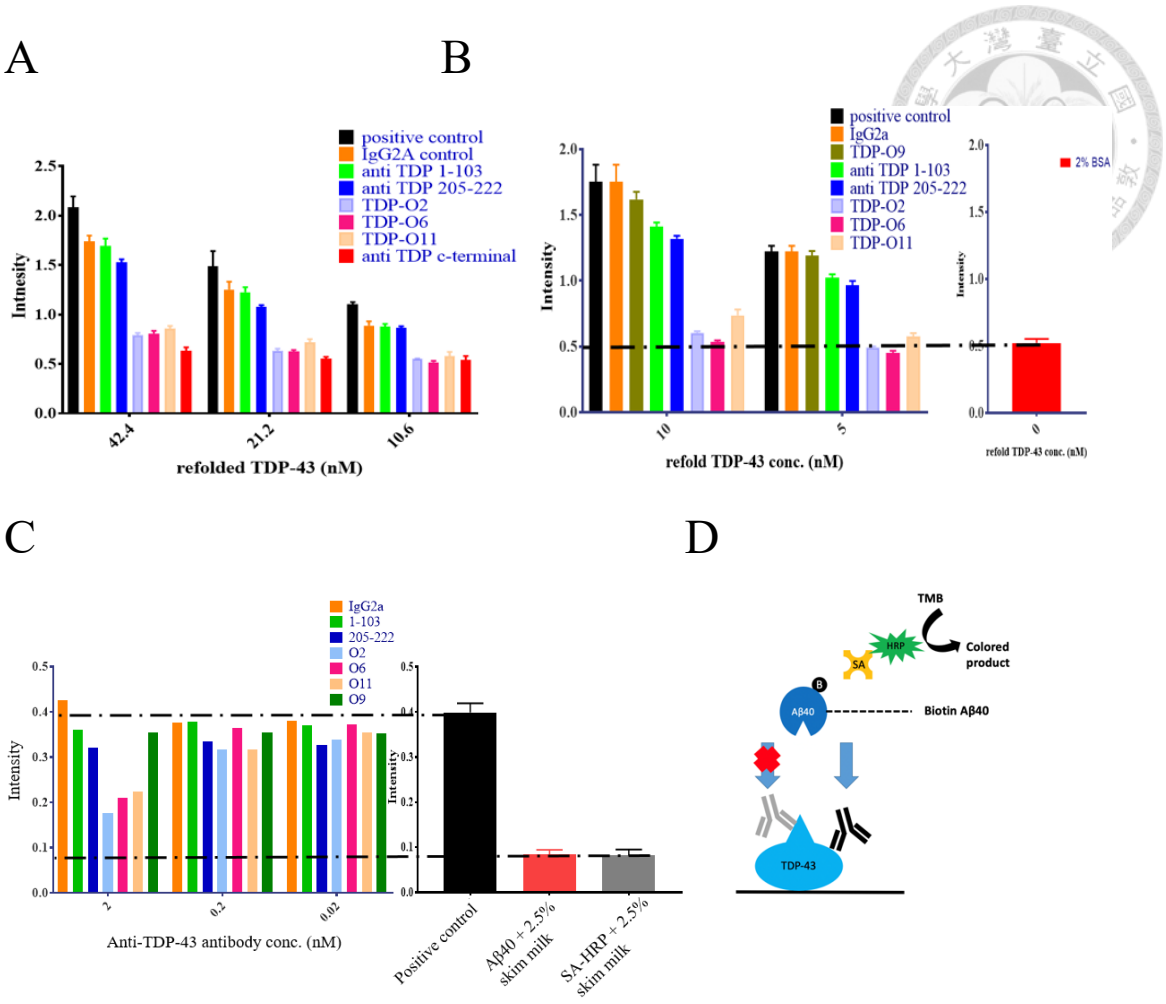

Figure 21. ELISA to investigate the binding site between Aβ40 and TDP-43. (A) Refolded TDP-43 was coated on ELISA plate in 10 mM Tris, pH 8.0. The blocking reagent was 2% BSA, which equaled to 300 μM BSA. The concentration of antibodies was 2 nM and biotin-Aβ40 was 0.25 μM. The ratio of secondary antibodies was 1:5,000. (B) The concentration of antibodies was 2.5 nM. The concentration of biotin-Aβ40 was 0.25 μM. (C) The blocking reagent was 2.5% skim milk. The concentration of refolded TDP-43 was 10 nM and the concentration of biotin-Aβ40 was 0.25 μM. (D) The cartoon figure of the experiment flowchart.

doi:10.6342/NTU201903526

References:

1. Thompson, C.A., et al., *Systematic review of information and support interventions for caregivers of people with dementia.* BMC Geriatrics, 2007. **7**(1): p. 18.
2. Wimo, A., et al., *The worldwide costs of dementia 2015 and comparisons with 2010.* Alzheimer's & Dementia, 2017. **13**(1): p. 1-7.
3. Bondi, M.W., E.C. Edmonds, and D.P. Salmon, *Alzheimer's Disease: Past, Present, and Future.* Journal of the International Neuropsychological Society, 2017. **23**(9-10): p. 818-831.
4. Du, X., X. Wang, and M. Geng, *Alzheimer's disease hypothesis and related therapies.* Translational Neurodegeneration, 2018. **7**(1): p. 2.
5. Haass, C. and D.J. Selkoe, *Soluble protein oligomers in neurodegeneration: lessons from the Alzheimer's amyloid β-peptide.* Nature Reviews Molecular Cell Biology, 2007. **8**: p. 101.
6. Shankar, G.M., et al., *Amyloid-β protein dimers isolated directly from Alzheimer's brains impair synaptic plasticity and memory.* Nature Medicine, 2008. **14**: p. 837.
7. Zhao, L.N., et al., *The Toxicity of Amyloid ß Oligomers.* International Journal of Molecular Sciences, 2012. **13**(6).
8. van der Kant, R. and Lawrence S.B. Goldstein, *Cellular Functions of the Amyloid Precursor Protein from Development to Dementia.* Developmental Cell, 2015. **32**(4): p. 502-515.
9. Gu, L. and Z. Guo, *Alzheimer's Aβ42 and Aβ40 peptides form interlaced amyloid fibrils.* Journal of Neurochemistry, 2013. **126**(3): p. 305-311.
10. Pauwels, K., et al., *Structural Basis for Increased Toxicity of Pathological Aβ42:Aβ40 Ratios in Alzheimer Disease.* Journal of Biological Chemistry, 2012. **287**(8): p. 5650-5660.
11. Chen, G.-f., et al., *Amyloid beta: structure, biology and structure-based therapeutic development.* Acta Pharmacologica Sinica, 2017. **38**: p. 1205.
12. Balbach, J.J., et al., *Supramolecular Structure in Full-Length Alzheimer's β-Amyloid Fibrils: Evidence for a Parallel β-Sheet Organization from Solid-State Nuclear Magnetic Resonance.* Biophysical Journal, 2002. **83**(2): p. 1205-1216.
13. Ou, S.H., et al., *Cloning and characterization of a novel cellular protein, TDP-43, that binds to human immunodeficiency virus type 1 TAR DNA sequence motifs.* Journal of Virology, 1995. **69**(6): p. 3584.

doi:10.6342/NTU201903526

14. Buratti, E. and F.E. Baralle, *Characterization and Functional Implications of the RNA Binding Properties of Nuclear Factor TDP-43, a Novel Splicing Regulator ofCFTR Exon 9.* Journal of Biological Chemistry, 2001. **276**(39): p. 36337-36343.
15. Arai, T., et al., *TDP-43 is a component of ubiquitin-positive tau-negative inclusions in frontotemporal lobar degeneration and amyotrophic lateral sclerosis.* Biochemical and Biophysical Research Communications, 2006. **351**(3): p. 602-611.
16. Kabashi, E., et al., *TARDBP mutations in individuals with sporadic and familial amyotrophic lateral sclerosis.* Nature Genetics, 2008. **40**: p. 572.
17. Josephs, K.A., et al., *Staging TDP-43 pathology in Alzheimer's disease.* Acta Neuropathologica, 2014. **127**(3): p. 441-450.
18. Chanson, J.B., et al., *TDP43-Positive Intraneuronal Inclusions in a Patient with Motor Neuron Disease and Parkinson's Disease.* Neurodegenerative Diseases, 2010. **7**(4): p. 260-264.
19. Davidson, Y., et al., *TDP-43 in ubiquitinated inclusions in the inferior olives in frontotemporal lobar degeneration and in other neurodegenerative diseases: a degenerative process distinct from normal ageing.* Acta Neuropathologica, 2009. **118**(3): p. 359-369.
20. Mompeán, M., et al., *Point mutations in the N-terminal domain of transactive response DNA-binding protein 43 kDa (TDP-43) compromise its stability, dimerization, and functions.* Journal of Biological Chemistry, 2017. **292**(28): p. 11992-12006.
21. Lukavsky, P.J., et al., *Molecular basis of UG-rich RNA recognition by the human splicing factor TDP-43.* Nature Structural &Amp; Molecular Biology, 2013. **20**: p. 1443.
22. Cohen, T.J., V.M.Y. Lee, and J.Q. Trojanowski, *TDP-43 functions and pathogenic mechanisms implicated in TDP-43 proteinopathies.* Trends in Molecular Medicine, 2011. **17**(11): p. 659-667.
23. Davis, S.A., et al., *TDP-43 expression influences amyloidβ plaque deposition and tau aggregation.* Neurobiology of Disease, 2017. **103**: p. 154-162.
24. James, B.D., et al., *TDP-43 stage, mixed pathologies, and clinical Alzheimer's-type dementia.* Brain, 2016. **139**(11): p. 2983-2993.
25. Gu, J., et al., *TDP-43 suppresses tau expression via promoting its mRNA instability.* Nucleic Acids Research, 2017. **45**(10): p. 6177-6193.

doi:10.6342/NTU201903526

26. Fang, Y.-S., et al., *Full-length TDP-43 forms toxic amyloid oligomers that are present in frontotemporal lobar dementia-TDP patients.* Nature Communications, 2014. **5**: p. 4824.
27. LaFerla, F.M., K.N. Green, and S. Oddo, *Intracellular amyloid-β in Alzheimer's disease.* Nature Reviews Neuroscience, 2007. **8**: p. 499.
28. Wang, P., et al., *TDP-43 induces mitochondrial damage and activates the mitochondrial unfolded protein response.* PLOS Genetics, 2019. **15**(5): p. e1007947.
29. Querfurth, H.W. and F.M. LaFerla, *Alzheimer's Disease.* New England Journal of Medicine, 2010. **362**(4): p. 329-344.
30. Iguchi, Y., et al., *Exosome secretion is a key pathway for clearance of pathological TDP-43.* Brain, 2016. **139**(12): p. 3187-3201.
31. Gao, J., et al., *Pathomechanisms of TDP-43 in neurodegeneration.* Journal of Neurochemistry, 2018. **146**(1): p. 7-20.
32. Hawe, A., M. Sutter, and W. Jiskoot, *Extrinsic Fluorescent Dyes as Tools for Protein Characterization.* Pharmaceutical Research, 2008. **25**(7): p. 1487-1499.
33. Ni, C.-L., et al., *Folding stability of amyloid-β 40 monomer is an important determinant of the nucleation kinetics in fibrillization.* The FASEB Journal, 2011. **25**(4): p. 1390-1401.
34. Tjernberg, L.O., et al., *Amyloid β-peptide polymerization studied using fluorescence correlation spectroscopy.* Chemistry & Biology, 1999. **6**(1): p. 53-62.
35. Xue, C., et al., *Thioflavin T as an amyloid dye: fibril quantification, optimal concentration and effect on aggregation.* Royal Society Open Science. **4**(1): p. 160696.
36. Kumar, S., et al., *Foldamer-Mediated Structural Rearrangement Attenuates Aβ Oligomerization and Cytotoxicity.* Journal of the American Chemical Society, 2017. **139**(47): p. 17098-17108.
37. Janowska, M.K., K.-P. Wu, and J. Baum, *Unveiling transient protein-protein interactions that modulate inhibition of alpha-synuclein aggregation by beta-synuclein, a pre-synaptic protein that co-localizes with alpha-synuclein.* Scientific Reports, 2015. **5**: p. 15164.
38. Fezoui, Y., et al., *An improved method of preparing the amyloid β-protein for fibrillogenesis and neurotoxicity experiments.* Amyloid, 2000. **7**(3): p. 166-178.
39. Hou, L., et al., *Solution NMR Studies of the Aβ(1−40) and Aβ(1−42) Peptides Establish that the Met35 Oxidation State Affects the Mechanism of Amyloid*

doi:10.6342/NTU201903526

Formation. Journal of the American Chemical Society, 2004. **126**(7): p. 1992-2005.

40. Hou, L. and M.G. Zagorski, *NMR Reveals Anomalous Copper(II) Binding to the Amyloid Aβ Peptide of Alzheimer's Disease.* Journal of the American Chemical Society, 2006. **128**(29): p. 9260-9261.
41. Afroz, T., et al., *Functional and dynamic polymerization of the ALS-linked protein TDP-43 antagonizes its pathologic aggregation.* Nature Communications, 2017. **8**(1): p. 45.
42. Reyes Barcelo, A.A., F.J. Gonzalez-Velasquez, and M.A. Moss, *Soluble aggregates of the amyloid-β peptide are trapped by serum albumin to enhance amyloid-β activation of endothelial cells.* Journal of Biological Engineering, 2009. **3**(1): p. 5.

doi:10.6342/NTU201903526